Development patterns of an oligo-mesophotic isolated carbonate buildup (Upper Burman Limestone, Lower Miocene, Yadana field, offshore Myanmar)

Thomas TEILLET [1,2], *François FOURNIER* [1], *Lucien F. MONTAGGIONI* [1], *Marcelle BOUDAGHER-FADEL*[3], *Jean BORGOMANO* [1], *Juan C. BRAGA* [4], *Quentin VILLENEUVE* [1], *Fei HONG* [2]

[1] : Aix-Marseille Université, CNRS, IRD, Cerege, Um 34, 3 Place Victor Hugo (Case 67), 13331 Marseille Cedex 03, France[2] : TOTAL, CSTJF, Avenue Larribau, 64000 Pau, France

[2]: TOTAL, CSTJF, Avenue Larribau, 64018 Pau Cedex, France

[3]: Postgraduate Unit of Micropalaeontology, Department of Geological Sciences, University College London, Gower Street, London WC1E 6BT, U.K.

[4] : Universidad de Granada, Avenida de la Fuente Nueva 18071 Granada, Spain

Abstract

The development history of a strictly oligo-mesophotic, Lower Miocene, isolated carbonate platform in the northern Andaman Sea (Yadana platform) has been evidenced from the integration of sedimentological core studies, well-correlations, seismic geomorphology and analysis of the ecological requirements of the main skeletal components. Three types of carbonate factory operated on the top of the platform, depending on the paleoceanographic setting: 1) a scleractinian-echinodermal carbonate factory developing under meso-oligophotic, and high-nutrient

(mesotrophic to eutrophic) conditions, 2) a large benthic foraminiferal (LBF)-coralline algal carbonate factory prevailing under mesophotic and oligotrophic conditions and 3) a LBF carbonate factory dominating in oligophotic and oligotrophic settings. The low lateral changes in facies, the layer-cake depositional architecture inferred from well-correlations and the seismic expression of the Yadana buildup suggest a deposition on a flat shelf. Carbonate production and accumulation on the Yadana platform has been shown to be mainly controlled by light intensity, nutrient content and water energy. Corals have been shown to preferentially develop in low-light and high-nutrient setting and are accompanied by abundant communities of suspension-feeders such as ophiuroids. Changes in monsoonal intensity and terrestrial runoff from the river Irrawaddy during the Early Miocene, are likely responsible for the repeated development of high-nutrient, low-to-moderate water transparency conditions as well as for the episodic occurrence of upwelling currents and/or internal waves, that promoted the development of an oligo-mesophotic, incipiently drowned platform.

1. Introduction

Prolific sedimentological litterature regarding tropical Cenozoic carbonate systems from South-East Asia have revealed a great diversity of carbonate factories in relation to a wide range of global and local environmental and climatic parameters such as temperature, nutrient content, light penetration and terrigenous inputs (Madden & Wilson, 2013; Wilson, 2002, 2008). Usually, the concept of 'tropical carbonate factory' is associated with a dominantly biological carbonate production in warm, well-illuminated, oligotrophic, and very shallow waters (Hallock & Glenn, 1986; Pomar & Hallock, 2008; Schlager, 2000; Schlager, 2003). In such settings, carbonates are typically produced by various photosynthetic autotrophs including calcareous green and red algae,

and by organisms with photosynthetic symbionts such as zooxanthellate corals and large benthic foraminifera (LBF), thus resulting in the so-called Photozoan sediment association (James, 1997). The humid tropical environments are characterized by a wide range of clastic sediment, fresh water and nutrients inputs that are generally considered unfavorable to the photozoan carbonate production (e.g. Schlanger, 1989; Wilson, 2002, 2008). Many modern and Cenozoic, equatorial, south-east Asian carbonate systems are associated with upwelling and/or terrestrial runoff, high turbidity and cool waters (Madden & Wilson, 2013). In such settings, nutrient-reliant biota often outweighs light dependent autotrophs (Tomascik *et al.*, 2000; Wilson & Vecsei, 2005). At regional scale, the combined effect of high nutrient supplies and low light penetration promotes the development of large scale isolated and/or land-attached oligophotic (*sensu* Pomar, 2001) platforms such as the modern Paternoster platform (Burollet *et al.*, 1986), Spermonde platform (Renema & Troelstra, 2001), Kalukalukung banks (Roberts & Phipps, 1988) and the Cenozoic Berai (Saller & Vijaya, 2002), Tonasa (Wilson & Bosence, 1996) , Melinau platforms (Adams, 1965) and foreslope of Hawaiian Islands (Pyle *et al.*, 2016). However in such carbonate platforms, even though oligophotic carbonate production dominates, reefal and/or non-reefal euphotic carbonate factories are coexisting (Wilson & Vecsei, 2005). The reconstruction of depositional models for ancient, coral-rich sedimentary systems has become a major issue in carbonate sedimentology since significant oligo-mesophotic scleractinian carbonate factories have been evidenced in modern and Cenozoic environments (e.g. Kahng *et al*. 2010; Lesser *et al*., 2009; Morsilli *et al*. 2012), thus questioning the common use of 'tropical carbonate factory' concepts in paleoenvironmental interpretations.

The Oligo-Miocene Yadana carbonate platform is located in the Andaman sea, offshore Myanmar. Three-dimensional seismic interpretation of the Yadana gas-bearing carbonate reservoir revealed

that the upper part of the Yadana (Upper Burman Limestone: UBL, Lower Miocene) platform is an isolated carbonate buildup developing on top of a land-attached system (Paumard et al. 2017). The analysis of seismic facies coupled with the use of classical 'tropical carbonate factory' concepts have led to interpret the UBL Yadana buildup as a euphotic reef-rimmed carbonate platform (Paumard et al. 2017). The present study, on the basis of a detailed analysis of biological associations, sedimentological and diagenetic features from cores, aims at 1) revising the depositional model of the UBL Yadana platform, 2) interpreting the depositional paleoenvironments in terms of turbidity, light penetration, hydrodynamic energy and nutrient availability, and 3) documenting the development of a coral-rich carbonate platform in oligo-mesophotic conditions, in south-east Asia during the Early Miocene.

2. Geological setting

During the Cenozoic, the regional geodynamic context strongly controlled the initiation, the development and the demise of SE Asian carbonate systems (Wilson & Hall, 2010). As a result of the oblique collision of the Indian-Australian plate beneath the Eurasian plate, the Sunda subduction zone formed during the Early Eocene (Chakraborty & Khan, 2009; Curray, 2005), and induced the opening of the Andaman Sea as a back-arc basin (Fig. 1). During the Oligocene to the Early Miocene, the Yadana carbonate buildup developed at top of a volcanic arc (Racey, 2015), located in the northern Andaman Sea, and separating the M5 fore-arc basin to the West from the Moattama back-arc basin to the East (Fig. 2). A long-term hiatus in deposition (~15 Myr) occurred from the Early Miocene to the Late Miocene and the UBL carbonates are sealed by Late Miocene (N16 planktonic zone) pro-delta shales (Pyawbwe and Badamyar formations) from the Irrawaddy

deltaic system (Paumard *et al*., 2017). During the Late Miocene, the separation between the Indian and Australian plates resulted in a regional compression and eastward in the Andaman basin opening and tilting of the Yadana high (Curray, 2005). At present, as a result of such an eastward tilting, the Yadana gas accumulation is located on the structurally elevated western margin of the Oligo-Miocene carbonate buildup.

The base of the lithostratigraphic regional chart (Fig. 3) includes Upper Eocene volcano-clastics sediments. Above has developed the Oligo-Miocene carbonate platform, reaching up to 700 m thick, this can be divided into two parts. The lower Burman Limestone formation (LBL), Chattian in age (Paumard *et al.*, 2017) consists of two distinct carbonate buildups separated by a central canyon. The central canyon is filled by the Sein clastic formation (late Chattian after Paumard *et al. 2017)*. Above the LBL carbonate buildups, the Upper Burman Limestone formation (UBL) occurs as a single carbonate buildup during the Early Miocene and interpreted as a . It corresponds to the main gas-bearing reservoir. The Yadana carbonate buildup arranges from 25 km to 30 km in size. The investigated cored interval covers the uppermost 150 meters of the UBL formation in the western part of the buildup (gas field).

3. Material and Methods

Approximately 20 wells have penetrated the top of the Upper Burma Limestone. Four wells (YAD-1, YAD-2, YAD-3 and YAD-4), located in the western half of the buildup (Fig. 2), have been selected in this study for a detailed sedimentological study. A total of 343 m has been investigated in the present work (YAD-1: 87.5 m, YAD-2: 84 m YAD-3: 59.5 m YAD-4: 112 m). The relevant

cores are described in terms of textures and biological attributes. Detailed microscopic examination of 700 thin-sections provided the backbone of microfacies analysis identification. Thin-sections have been stained with blue colored epoxy resin for porosity evaluation and with Alizarin Red to differentiate dolomite from calcite.

The studied dataset includes 2D and 3D seismic surveys acquired by TOTAL. The prestack time migrated data have a vertical resolution of around 20 m within the carbonates. Amplitude and seismic attributes (coherency) have been used to highlight macro-scale platform morphology. In addition to the gas water contact (GWC) that forms a well-identified flat-spot, 5 key- seismic reflectors respectively named TOP UBL, H9, H9A, H10B and H10 have been interpreted within the carbonate buildup.

Petrographical analysis of thin sections combined with identification of sedimentary structures, depositional textural and biological assemblages in cores, has allowed distinct facies to be recognized. These facies have been interpreted in terms of depositional environments by reference to modern and ancient analogues. The biological composition of carbonate rocks has been quantified by using point-counting on thin-sections. The Yadana carbonates have been chronologically constrained using benthic and planktonic foraminiferal stratigraphy relative to the biostratigraphical time scale (as defined by Gradstein *et al.* 2012). The benthic foraminiferal stratigraphy was based on the East Indian Letter Classification (Adams, 1970; BouDagher-Fadel, 1999; BouDagher-Fadel, 2008, 2015). The planktonic foraminiferal biostratigraphy was based on the zonation defined by (Berggren *et al*., 1995) and modified by (Wade *et al.*, 2011). The paleoenvironmental reconstructions are based on paleoecological interpretations of the identififying biotic assemblages, including coralline algae and large benthic foraminifers.

4. Results

4.1 Biostratigraphy

The chronostratigraphic framework of the Yadana carbonate buildup has been revised (Fig. 4) on the basis of: 1) a reappraisal of the available planktonic and benthic foraminiferal biostratigraphy, and 2) new taxonomic determinations of the benthic foraminiferal material from the studied UBL cores (Fig. 5). The ages are based on the first appearance of planktonic and shallow benthic foraminifera, and of the letter stages after BouDagher-Fadel (2008) and BouDagher-Fadel (2015) and relative to the biostratigraphical time scale, as defined by Gradstein *et al*. (2012).

The Upper Burma Limestone (UBL) overlies the Sein siliciclastics of late Rupelian to early Chattian age as derived from the occurrence of *Paragloborotalia opima* (P20-P21). The lower part of the UBL limestones (below the cored interval) is poorly constrained in terms of age of deposition. The lowermost cored interval from the UBL is early Aquitanian in age (N4a) as supported by the first co-occurrence of *Miogypsina gunteri* and *Miogypsinoides formosensis* (YAD-1, 1340.06m). The uppermost UBL limestone is recognized to be Burdigalian in age (N6) on the basis of the occurrence of *Miogypsina intermedia, Miogypsina globulina* and *Miogypsinoides dehaarti* (YAD-2 1272.23m)

Calcareous nannofossils and planktonic foraminifers present in the pro-delta shales overlying the UBL (*Discoaster quinqueramus, Sphaeroidinellopsis seminulina, Globigerinoides extremus*) are assigned to the Tortonian (N20-N17), thus suggesting a time hiatus of approximatively 15 My at top of the Yadana platform.

4.2 Lithofacies and paleo-environmental interpretations

Carbonate rocks from the UBL interval are dominantly calcite-dominated limestones, sometimes with low proportions of dolomite (<10%). Quartz grains are extremely rare. In decreasing order of abundance the main biological components observed on thin sections are: (1) non-geniculate coralline algae (18% on average; YAD-1=22.5% ;YAD-2=18% ;YAD-3=18% ;YAD-4=13%), (2) large benthic foraminifera and (17% on average; YAD-1=19.5% ;YAD-2=17% ;YAD-3=17%;YAD-4=16%), (3) corals(7% on average; YAD-1=4% ;YAD-2=9% ;YAD-3=5% ;YAD-4=10%). Subordinates components include echinoderms (5% on average), bryozoans, green algae and planktonic foraminifera. Five distinct lithofacies have been defined and interpreted in terms of depositional environments (Table 1):

LF1. Coralline algal floatstone to rudstone (Fig. 6A to 6G)**:**

The coralline algal floatstones to rudstones consist of spheroidal-ellipsoidal rhodoliths or pieces of branching coralline algae embedded within a coralline algal-foraminiferal wackstone to packstone matrix. The coralline algal association is composed of *Lithothamnion, Mesophyllum* and *Sporolithon.* Rhodoliths are heterometric, mostly with diameters ranging from 1 cm to 10 cm and commonly displaying warty and branching growth forms. Loose pieces of branching and columnar coralline algae (particularly *Lithothamnio*n and *Sporolithon*) may be dominant in some intervals. Loose and hooked *Mesophyllum* are present in very low amount. The foraminiferal assemblage is dominated by *Spiroclypeus tidoenganensis* and *Nephrolepidina sumatrensis*, with common occurrences of *Miogypsinoides*, *Miogypsina* and *Heterostegina* (*Vlerkina*). Echinoderms, ectoprocts and planktonic foraminifera are occasional.

Interpretation: In LF1 facies, the coralline algal assemblage is dominated by the melobesioids *Lithothamnion, Mesophyllym* and *Sporolithon.* Such an association is typical of low-light environments, in oligo-mesophotic setting (Braga, 2010). In contrast, mastophoroids typical of euphotic, reefal environments, are extremely rare or lacking. In modern, tropical, low-turbidity environments, melobesioids are have been shown to occur preferentially at water-depths ranging from 30 to 80 m (Braga & Aguirre, 2004). The co-occurrence of warty rhodoliths and pieces of branching coralline algae belonging to the same taxa may suggest that the isolated branches may derive from the fragmentation of branching rhodoliths during high-energy events such as storms or internal waves (Bosence, 1983; Freiwald *et al*., 1994). The foraminiferal assemblage dominated by large and flat *Spiroclypeus* and L*epidocyclinids* is typical of oligo-mesophotic environments, at water depths of 30 m or greater , but could live comfortably at minimum of 70 m (Hallock & Glenn, 1986; Hine, 2001; Noad, 2001; Saller, 1993). In contrast, the benthic foraminifers *Miogypsinoides dehaarti* and *Heterostegina* (*Vlerkina*) *borneensis* are common taxa in shallow-water, euphotic environments. These forms are sometimes associated with sea-grass beds (BouDagher-Fadel, 2008; Fournier *et al.*,, 2004; Hallock & Pomar, 2012; Maurizot *et al*., 2016) but were also reported from shallow mid-ramp environments (Bassi, 2005; Bassi *et al.*, 2007; Rahmani *et al.*, 2009). The high micrite matrix content strongly suggests that the depositional environment of LF1 was relatively sheltered or not permanently subject to wave-action. As a consequence, the biological and textural features of LF1 facies likely reflect a deposition in the shallowest part of the mesophotic zone, in an area located below the base of permanent wave action but experiencing to episodic high-energy events.

LF2.1. Large benthic foraminiferal rudstone (Fig.s 7A & 7B):

The LF2.1 facies consists in relatively thin (<1m) accumulations of large benthic foraminifers (LBF), enriched in red algal fragments, with rare ectoproctes echinoderms. The intergranular spaces may be occupied by a peloidal grainstone matrix or occluded by sparry calcite cements. Large benthic foraminifera are usually pluri-centimetric in size (up to 2cm), these commonly disorentied form layers .Most of them display shocking and reworking imprints on their edges. The foraminiferal assemblage is dominated by *Lepidocyclina* (*Nephrolepidina*) *sumatrensis, L.* (*N.*) *oneatensis,* and *Spiroclypeus tidoenganensis* with rarer specimens of *Amphistegina, Heterostegina, Miogyspina,* and *Miogypsinoides*. Coralline algae mainly include branching and encrusting, warty *Lithothamnion*, laminated, loose *Mesophyllum* and branching *Sporolithon.* At the scale of core and thin-section, the LF2.1 rudstone intervals are structureless (Fig. 7B).

Interpretation: The foraminiferal assemblage, dominated by *Nephrolepidina* and *Spiroclypeus* as well as the coralline algal association (*Lithothamnion-Mesophyllum-Sporolithon*) suggest that carbonate grains have been produced within the mesophotic zone (Braga *et al.*, 2010). Considering the probable low water turbidity due to the localtion of the platform far from potential terrigneous sources, this zone is likely regarded as having occurring below the action of surface waves. Nevertheless, the lack or scarcity of mud matrix in intergranular spaces, with the poor state of preservation of large benthic foraminifers, suggest episodic turbulence, strong enough to winnow mud and to rework and the large foraminiferal tests. The rare occurrence of *Amphistegina, Heterostegina, Miogyspina,* and *Miogypsinoides,* compared to LF1, may reflect that the LBF rudstones deposited at greater depths within the oligo-mesophotic zone. The muddy, together with the random layout pattern of the LBF may indicate that deposition operated during high-energy events (Pomar *et al*., 2015).

LF2.2. Large benthic foraminiferal floatstone (Fig. 7C & 7D).

LF2.2 lithofacies consists of large benthic foraminiferal floatstone with a coralline algal wackestone/packstone matrix. Large benthic foraminifers are up to 2cm in diameters,, thin-shelled, commonly well-preserved (unbroken), and typically horizontally-oriented. The foraminiferal assemblage is dominated by *Spiroclypeus tidoenganensis* with common occurrences of *Cycloclypeus, Eulepidina, Nephrolepidina. Miogypsinoides* and *Amphistegina.* Planktonic foraminifersoccur occasionally in LF2.2 lithofacies. Laminar and loose *Mesophyllum*, together with branching *Lithothamnion* are common components.

Interpretation: The foraminiferal assemblage dominated by very large and flat *Spiroclypeus, Cycloclypeus* and *lepidocyclinids*, is typical of oligophotic environments, depths of 30 m or greater, but could grow comfortably at depths as great as 70 m (Hallock & Glenn, 1986; Noad, 2001; Saller, 1993). The occurrence of planktonic foraminifera in LF2.2 is consistent with such water depths. The coralline algal assemblage, dominated by *Mesophyllum* and *Lithothamnion*, is also indicative of relatively low light conditions (e.g. Adey WH 1979; Bosence 1983; Rosler *et al.* 2015). The biological composition together with the well preservation state of flat-shaped LBF and the high proportion of micrite matrix strongly suggest that the LBF floatstones deposited in an oligophotic, low-energy environment.

LF3.1 Coral floatstone with echinoderm-rich wackestone matrix (Fig. 8 & 9)

LF3.1 lithofacies is a scleractinian floatstone consisting of thin branches of unidentified corals or massive fragments of Faviids and Pocilloporids. Associated forms included solitary corals. All are embedded in a wackestone matrix dominated by echinodermal fragments (mainly ophiuroids and

some echinoids), small pieces of non-articulated coralline algae and occasional benthic foraminifers (mainly broken lepidocyclinids and *Spiroclypeus*). The coralline algal assemblage is prominently composed of *Mesophyllum* and *Lithothamnion*. Within the UBL limestone, LF3.1 has been encountered in four distinct, 5 to 10 meter-thick intervals. LF3.1 lithofacies commonly exhibits intraclasts and brecciated intervals (Fig.9). In such brecciated intervals, grains are gravel to pebble-sized (typically 0.5-5 cm), angular, weakly reworked and do not exhibit evidence of dissolution. The inter-intraclast spaces are filled with a micrite containing various percentages of fine-grained echinoderm fragments. The top of LF3.1 intervals are characterized by uneven, tightly indurated, brecciated and bored surfaces (YAD-3 1295.5 on Fig. 9E). Early dissolution of aragonitic bioclasts (e.g. moldic cavities of coral) is also a common feature in the LF3.1 facies. Most of the residual leached corals are filled with a microbioclastic micrite that is identical in nature and in physical continuity with the matrix in which they are embedded (faint ghost fabrics *sensu* Sanders 2003).

Interpretation:

The nature of the biological assemblage in LF3.1 floatstone matrix, dominated by echinoderms and containing low amount of light-dependent biota, is not consistent with deposition under euphotic conditions. The benthic foraminifers (mainly lepidocyclinids and *Spiroclypeus*) are scarce, thus likely reflecting oligo-mesophotic conditions. In addition, the red algal assemblage (*Mesophyllum* and *Lithothamnion*) is similar to that of the LF1 and LF2 facies. The importance of coral-dominated carbonate factories in oligo-mesophotic settings has been recognized in various Cenozoic carbonate systems, in relation to nutrient-rich and episodically agitated environments (Mateu-Vicens *et al.* 2012; Morsilli *et al*. 2012; Pomar *et al.* 2014). Under such conditions, corals

may significantly develop by enhancing their heterotrophic strategy acting as suspension feeders (e.g. Morsilli *et al*. 2012). It is not excluded that corals, usually present in the form of fragments of colonies or solitary corals, may have derived from nearby patches. The relative dominance of heterotrophs (echinoderms) and scarcity of light-dependent large benthic foraminifers and coralline algae could be interpreted as being related to increasing water-depth or water-turbidity but also to an increasing nutrification. In ancient and modern environments, occurrences of dense populations of ophiuroids are regarded as requiring the combination of three conditions (Aronson, 2009; Aronson *et al.*, 1997): low skeleton-crushing predation, low rates of sediment resuspension and high flux of particulate organic matter. In brecciated and intraclastic intervals, the similarity between the texture and composition of the intraclasts and those of the matrix in which they are embedded, together with the lack of dissolution features at their edges, strongly suggest that early marine lithification and brecciation have operated coevally. The occurrence of boring features at top of LF3.1, together with early lithification and brecciation features are indication of low sedimentation rates and significant periods of non-deposition. The high micrite mud content in LF3 lithofacies is indicative of deposition in a low-energy setting, below wave-base. Nevertheless, episodic high energy events are needed to: 1) break up and removed coral colonies, the large benthic foraminifers and red algal crusts, 2) provide water turbulence sufficient enough for corals to thrive (e.g. Atkinson & Bilger 1992; Pomar *et al.* 2012; Pomar & Hallock 2008) and 3) trigger sediment brecciation and intraclast reworking on the early-lithified sea-bottom in process of cementation (Bouchette et al. 2001; Seguret et al. 2001). As a consequence, LF3 lithofacies is interpreted to have deposited in a low-energy oligo-mesophotic, nutrient-rich (mesotrophic to eutrophic?) environment that is subjected to episodic high-energy events.

LF3.2 Echinodermal wackestone (Fig. 8D & 8F)

The LF3.2 lithofacies is a bioclastic wackestone dominated by pieces of echinoderms, including ophiuroid ossicles and echinoids. Small-size (<1mm) fragments of coralline algae (*Mesophyllum* and *Lithothamnion)* are common. Isolated coral pieces and rare fragments of large benthic foraminifers may be present. LF3.2 facies commonly occurs as layers interbedded within LF3.1 coral floatstones.

Interpretation:

As for LF3.1, the dominance of heterotrophs and the scarcity of light-dependent biota is believed to indicate a deposition within a low-light and/or nutrient-rich environment. The wackestone texture is indicative of low energy setting. The similarity in texture and biota between the echinodermal wackestone (LF3.2) and the matrix of the coral floatstone (LF3.1) strongly suggest that LF3.2 represents a lateral analog of LF3.1. This contention is reinforced by the fact that LF3.2 and LF3.1 form repeated thin-scale (0.10 to 1 m) alternations. Since LF3.1 and LF3.2 essentially differ in their coral abundance, they may reflect a gradient of proximity to coral patches.

4.2 ***Vertical and lateral changes in lithofacies and related environments***

Vertical changes in lithofacies, related depositional environments and notable surfaces are summarized in Fig. 10 & 11 for each well in the cored intervals of the UBL limestone. The intra-formational emersion origin of the remarkable surfaces is not obvious and all of the lithofacies have been interpreted as being deposited in oligo-mesophotic environments. In the cored sections the UBL limestone exhibits alternations of meter-to-decameter-scale sedimentary units dominated either by LF1, LF2.1 and LF2.2 facies (units O1 to O6: oligo-mesophotic and oligotrophic

environments) or by LF3.1 and LF3.2 facies (units ME1 to ME5: meso-oligophotic and meso-eutrophic settings). Transition between facies are mainly gradual consisting in the progressive variation of biological constituent proportions. However, the upper-part of coral-rich intervals (LF3.1 facies) is typically brecciated and topped by erosional surfaces (Fig. 9E, 10B& 10D). The intraclasts consist of fragments of coral floatstone (LF3.1) and display low displacement. They are embedded within an echinoderm-rich wackstone matrix, thus suggesting early lithification and early brecciation of the coral floatstone. The top of these brecciated intervals is commonly bored and is sharply overlain by LF1 or LF2.1 facies (Fig. 9A). Considering the deposition in a persistent oligo-mesophotic environment and because of the lack of emersion evidences, the surfaces of the UBL limestone occurring at the top of LF3 intervals (Figure 9E, 10D) are therefore interpreted as hardground surfaces that formed during periods of non-deposition. The well-correlation framework (Fig. 12) has been defined on the basis of: 1) the available LBF-based biostratigraphy, 2) the well-to seismic tie (vertical resolution ~10m), and 3) the correlation of oligo-/mesophotic and oligo-/meso-eutrophic cycles. The well-to-seismic tie revealed that the seismic reflectors roughly follow lithostratigraphic boundaries. For instance, the seismic marker H9B matches with the boundary between a lower, 10 meters-thick interval of foraminiferal wackestones (LF2.2) and an upper, massive, interval containing rhodoliths, lepidocyclinids and *Spiroclypeus* (LF1). The stratigraphic correlation between wells reveals a lack of significant lateral change in lithofacies within the carbonate buildup. Such a layer-cake architecture suggesting the lack of significant topographic gradient on top of the buildup. The cored section of the UBL limestone (Aquitanian-Burdigalian) exhibits five main coral floatstone (LF3) intervals with good cross-correlation.

4.3 Seismic geomorphology and seismic facies

The 3D seismic records from, the UBL interval are characterized by a set of flat, continuous, parallel, low to moderate amplitude reflectors (Fig. 13). There is no change in seismic facies or reflector morphology on the edges of the Yadana platform that could be interpreted as suggesting to the presence of reef barriers. The inter-well correlation of seismic markers is supported by the good lateral continuity of the seismic reflectors within the UBL limestone (Fig. 13A & 13B). The lack of significant lateral changes in amplitude, the flat morphology and the parallel pattern of the reflectors are strongly consistent with a layer-caked stratigraphic architecture (low changes in lateral lithofacies and thickness) as suggested by the well correlations (Fig. 12), variations in thickness within the coral-rich units (<10m) are below or similar to the vertical resolution of seismic (~20m).

On the seismic profiles, reflectors from the UBL appear sharply truncated at the western margin (Fig. 13C). In addition, the very irregular shape of the UBL top surface on isochron and coherency maps (Fig. 13E & 13F) argues for a significant erosion of the Yadana buildup, after the Burdigalian and prior to deposition of the overlying prodelta shales during the Tortonian. Coherency map of the top UBL surface highlights circular depressions (sinkholes?) and sinuous incisions that could be interpreted as incised valleys or karst collapse features (Fig. 13E & 13F).

5. DISCUSSION

The Yadana buildup: an example of an Early Miocene, isolated, oligo-mesophotic carbonate platform

Previous interpretations (Paumard *et al.*, 2017) of the Yadana carbonate platform have been based on the modern, shallow-water, euphotic and oligotrophic barrier-reef-lagoon model. The present

environmental interpretations are based on: 1) interpretations of the skeletal components and the ecological requirements of the benthic communities from which they have derived, particularly light for autotrophs and food requirements for heterotrophs, 2) rock textures as indicative of water-energy, 3) reconstruction of sedimentary geometries based on well-correlations and seismic morphology.

The isolated nature of the Yadana carbonate system during the Aquitanian and Burdigalian (UBL Limestone) has been demonstrated by the three-dimensional interpretation of seismic data (Paumard *et al.*, 2017). The analyzed wells are all located in the western half of the buildup. The lateral correlative potential of the lithofacies and their variability in thickness are indicative of a weak topographic gradient, at least in the western part of the buildup. In addition, the carbonate sediments from the UBL are characterized by the absence of strictly euphotic constituents such as reef dwelling or seagrass-related biota. This suggests that the area close to the well area were not supplies from a source of sediments produced by a euphotic carbonate factory. In addition, the lack of lateral changes in the seismic facies and in thickness eastward, as revealed by the seismic data, supports the interpretation of a flat-topped platform for the whole Lower Miocene Yadana buildup.

The layer-caked architecture of the UBL limestone is indicating of low lateral changes in depositional environments on the platform top at a given time. In contrast, the vertical changes in lithofacies can be interpreted in terms of changing environmental parameters such as nutrient supplies, light-penetration, water energy and water-depth. The Upper Burma Limestone from the Yadana buildup has recorded three types of carbonate factory that operated on the top of the platform depending on the paleoenvironmental context: 1) a scleractinian-echinodermal carbonate factory developing under oligophotic, and high-nutrient (mesotrophic to eutrophic) conditions, 2)

a LBF-coralline algal carbonate factory prevailing under mesophotic and oligotrophic conditions and 3) a LBF carbonate factory dominating in oligophotic and oligotrophic settings.

The scleractinian-echinodermal carbonate factory (Fig. 14A)

The isolation of the Yadana platform, the lack of euphotic constituents within LF3.1 and LF3.2, the relative scarcity of coralline red algae and benthic foraminifers, and the inter-well correlatability of the coral-rich intervals suggest that the scleractinian-echinodermal carbonate factory developed on top of a flat shelf located in the deeper part of the oligophotic zone. In modern environments, low-light coral communities are known to include both zooxanthellate and azooxanthellate corals and occur in the lower half of the photic zone at depths down to 150m (e.g. Kahng et al. 2010). In such environments, zooxanthellate corals may exhibit various photo-acclimatization strategies, but can also develop a heterotrophic behavior, as suspension feeders, particularly when light significantly decreases with increasing depth or increasing turbidity, or during periods of high nutrient supplies (Alamaru *et al.*, 2009; Chan *et al.*, 2009; Lesser *et al.*, 2009; Mass *et al.*, 2007; Morsilli *et al.*, 2012; Muscatine *et al.*, 1989). The abundance of ophiuroids in LF3.1 and LF3.2 facies suggest that the prevailing environmental conditions on top of the Yadana platform favored the development of suspension-feeders (McKinney & Hageman, 2007). In modern (see Kahng et al., 2010 and references therein) and ancient low-light environments, corals are known to form low-relief buildups such as in Late Eocene pro-delta environments from Spain (Morsilli et al., 2012). The strategy consisting in forming mounds is believed to favour the development of suspension feeders since such reliefs promote turbulent currents capable of carrying picoplanktons and phytoplanktons (Atkinson & Bilger, 1992; Hearn, Atkinson, & Falter, 2001; Morsilli *et al.*, 2012; L. Pomar & Hallock, 2008; Ribes *et al.*, 2003). In the Yadana platform,

corals from the LF3.1 facies are generally broken and possibly derive from neighboring patches or coral heads even though typical coral boundstones have never been encountered in the studied cores. Since LF3.1 and LF3.2 lithofacies mostly differ in their coral abundance, they may reflect a gradient of proximity to such a possible mounds. In addition, the lateral changes in thickness (<10m) of coral-rich units, as well as the lateral pinching out of some of these units, may advocate for the existence of localized sources of coral production, scattered on the Yadana shelf, promoting the formation of a mounded, uneven, top of platform morphology (Fig. 14A). The elevation of such possible mounds is probably far below the resolution of seismic (~20m) as shown by the fact that all seismic reflectors within UBL exhibit a continuous and flat morphology. The development of a scleractinian-echinoderm carbonate factory may have been favored by the upward mixing of deeper, nutrient-rich waters by means of upwelling or internal waves around the nutricline that typically occur in the lower part of the photic zone (Anderson, 1969; Renema & Troelstra, 2001; Steele & Yentsch, 1960). The high lime-mud content in LF3.1 and LF3.2 facies supports the interpretation of low energy environments, below the surface wave base. But the occurrence of carbonate breccias occurring at top of early lithified coral-floatstone intervals, together with the common fragmentation of corals, LBF and coralline algae are indicative of episodic high-energy events that could have been generated precisely around the nutricline by internal waves (Morsilli & Pomar, 2012). Finally, the early dissolution of coral aragonite (faint ghost texture of coral floatstones) is indicative of under-saturated conditions which is a common feature of cold, CO_2-rich waters from upwelling currents (Feely *et al.*, 2008). Additionally, enhanced organic matter decay coupled with respiration around the nutricline (L. Pomar & Hallock, 2008) may have accentuated the under-saturation effect with regard to aragonite on the Yadana platform top.

The LBF-coralline algal carbonate factory (Fig. 14B)

Foraminiferal and coralline-algal-dominated carbonate sediments (facies LF1 and LF2.1) are found in 10 to 25 metre-thick intervals that are correlatable between the studied wells. All of these biological constituents are indicative of mesophotic conditions. The lack of euphotic biota within such intervals strongly suggests that there has been no euphotic carbonate factory on the Yadana buildup at that time. The LBF-coralline algal carbonate factory, that was the source of carbonate sediment of LF1 and LF2.1 facies, is therefore interpreted to have operated on the top of the Yadana shelf, under mesophotic conditions. The abundance of light-dependent biota such as large and flat LBF suggest also low to moderate nutrient levels, likely oligotrophic, conditions (Hallock *et al*., 1991; Pomar *et al.*, 2017). The high lime-mud content in coralline algal floatstones LF1 strongly aadvocates for a low energy environment, below wave-action. However, the usual disintegration of branching rhodoliths and LBF argues for episodic occurrence of high-energy events. Another evidence of episodic high-energy events could be the occurrence of thin (<1m) beds of foraminiferal rudstones LF2.1 interbedded within coralline algal floatstones. The large dominance of LBF in LF2.1 may be related to a preferential sorting of low-density bioclasts during turbulent flow events in relation with storms or internal waves (Morsilli & Pomar, 2012). Subsequent bedload transportation and mass deposition of such coarse-grained sediments on the platform top resulted therefore in the formation of structureless bioclastic gravel bodies with non-oriented LBF tests.

The LBF carbonate factory (Fig. 14C)

Flat-shaped, large benthic foraminifers (*Spiroclypeus*, *Cycloclypeus* and *Eulepidina*) which are the dominant biota of LF2.2 facies are known to f characterize oligophotic environments (e.g. Beavington-Penney & Racey 2004; Buxton & Pedley 1989; Pomar *et al.* 2017). The dominance of light-dependent biota (LBF and more rarely coralline algae) suggest deposition with environments with low nutrient content. The lack of lateral changes in texture, biota and thickness between the wells for LF2.2 intervals in addition with the high lime-mud content is regarded as expressing a deposition on top of a low-energy flat shelf rather than on a ramp system.

Factors controlling carbonate production on the Yadana platform top

The vertical succession of distinct carbonate factories on the top of the Yadana platform during the Early Miocene is indicative of changes through time of three primordial parameters: 1) light intensity, 2) nutrient supplies and 3) hydrodynamics. Coral-echinodermal carbonate factories developed during periods of high nutrient supplies (meso-eutrophic conditions), in oligo-mesophotic settings. In contrast, coralline algal and foraminiferal-dominated carbonate factories are linked to oligotrophic and oligo-mesotrophic settings.

Light intensity in sea-water is a function of water-depth and extinction coefficient of light (e.g. Hallock & Glenn, 1986; Kahng *et al.* 2010) which is driven by a set of factors including terrigenous discharge, nutrient input, land-derived dissolved organic matter and plankton blooms. In addition, light-penetration has also been proved to be a function of latitude, the lower limit of photic zone deepening at low latitudes (Liebau, 1984). Under low turbidity conditions (extinction coefficient of light: 0.05), in open marine environments, the water depths of the oligo-mesophotic domain typically ranges from 30 to 130m (Pomar, 2001). In contrast, in most deltaic, higher

turbidity (extinction coefficient of light: 0.10) environments the oligo-mesophotic zone occurs between 15 and 70m (Morsilli *et al.,* 2012). The dominantly low-energy characteristics of the oligo-mesophotic deposits from the Yadana platform is consistent with a deposition below the fair-weather wave base (~20m). Changes with time from mesophotic to oligophotic carbonate factories on the Yadana platform top may be related either to a change of water depth, or to a change in water transparency.

In the case of an upward transition from the LBF-coralline-algal-dominated facies (LF1 and LF2.1) to the scleractinian-echinoderm facies (LF3.1 and LF3.2), the transition from a mesophotic to an oligophotic carbonate factory is coupled with a transition from oligotrophic to meso-eutrophic conditions. Such a transition (e.g: from units O1 to EM1 on Fig. 12) may suggest that the decrease in light intensity is related to an increase in nutrient supply and associated decrease in water transparency. The change from a mesophotic to oligophotic carbonate factory on top of the Yadana platform may therefore occur without any change in water-depth and does not necessary imply a rise in relative sea-level. Indeed, in modern settings, it is know that, chlorophyll and phaeophytin concentrations typically peak at the nutricline, coincides at the top of the pycnocline, which is located in the lower part of the photic zone where deeper nutrient-rich waters can mix upward owing to upwelling and internal waves ,where primary production is limited by poor light intensity (Hallock *et al.*, 1991; Morsilli *et al.,* 2012; Pomar *et al.,* 2011). An alternative interpretation would be that an upward transition from LBF-coralline-algal-dominated lithofacies to coral-echinodermal facies has resulted from an increase in water depth (and therefore in a relative sea-level rise), in turn making the top of the Yadana platform to coincide with the bathymetric range of the nutricline.

In contrast, an upward vertical change from LF2.2 (Large benthic foraminiferal floatstone facies) to LF1/LF2.1 (LBF-coralline-algal-dominated facies) are considered to be indicative of a transition from oligophotic to mesophotic environments, both with low nutrient concentrations and more likely accompanied by changes in water-depth. Such transitions occur within units O4 and O6 (Fig. 12).

Even though mud-supported fabrics dominate Yadana carbonate sediments and suggest deposition below the fair weather wave base, the occurrence of episodic high-energy events is supported by: 1) the occurrence of thin-beds of foraminiferal rudstone, 2) the common fragmentation of branching rhodoliths and flat-shaped LBF even in mud-supported sediments, and 3) the occurrence of brecciated intervals at top of early cemented coral-echinodermal facies. The action of storms would be the easiest way to explain the existence of high energy events in oligo-mesophotic environments located below the fair-weather wave base. However, the action of internal wave would also explain the occurrence of high-energy events and, in the case of the coral-echinodermal carbonate factory, would explain in the same time the high nutrient supplies (Pomar et al., 2011). The pycnoclines are considered to be preferential locations for suspension feeding metazoans to develop and to produce buildups since they are places of high nutrient concentrations and water agitation (Morsilli *et al.*, 2012; Pomar *et al.*, 2017). Thus, it is clear that the three fundamental parameters (nutrient content, light intensity, and hydrodynamics) controlling carbonate production on the Yadana platform are interdependent.

Origin of changes in nutrient supplies and light penetration

Nutrient supply in the Yadana buildup area may be potentially generated by terrestrial runoff or by upwelling currents. Now days, the Irrawaddy River of Myanmar is one of the muddiest rivers (Licht *et al.* 2016) in flowing into the northern Andaman Sea and the Gulf of Martaban *(Rao et al.,* 2005). It is the fifth largest river in the world in terms of suspended sediment discharge,known to have been the major source of sediment within the Andaman Sea since the Early Miocene (Licht *et al.,* 2016). As a consequence, the Gulf of Martaban is one of the largest perennially turbid zones of the world's oceans. The suspended sediment levels and the area covered by the highly turbid zone have been shown to be strongly governed by to spring-neap tidal cycles (Ramaswamy *et al.*, 2004). South of the Gulf of Martaban, in the Andaman Sea, around the location of the Yadana field, the nutrients supplied by the Irrawaddy river favor high concentrations of chlorophyll from algae and diatoms in the ocean (Ramaswamy *et al.,* 2004). The Late Oligocene and Early Miocene paleogeography of the Andaman Sea is quite similar to the modern (Fig. 1A et 1B). Changes over time in sediment and nutrient inputs from the Irrawaddy River have most likely controlled changes in water turbidity and nutrient concentration in the Yadana area. Periods of high terrigenous inputs may have driven the development of an oligophotic and meso-eutrophic carbonate factory, dominated by suspension feeders (corals and ophiuroids), at relatively shallow water-depth (10-50m).

Related to the global warming occurring during the Early Miocene and continuing until the Middle Miocene Optimum climatic (MMOC), the South Asian Monsoon (SAM), one of the most significant climatic components in the area is known to have occurred as early as the Oligocene-Miocene boundary (Fig. 4B) (Betzler *et al.*, 2018; Clift *et al.*, 2008; Clift & Vanlaningham, 2010). At present, theAndaman Sea, monsoonal activity is known to induce the formation of seasonal upwelling currents, particularly on the margin of Thailand (e.g. Chatterjee *et al.,* 2017). Seasonal

upwelling currents, related to monsoonal activity, have been also reported to occur during the Late Miocene in the Andaman Sea (Chakraborty & Ghosh, 2016).

The integration of various geochemical and mineralogical proxies by Clift et al. (2008) led to the conclusion that monsoon intensification started during the early Miocene (after ~24 Ma) and that at least 5 cycles of chemical weathering intensity have been recorded during the Aquitanian-Burdigalian interval. Changes in monsoonal activity during the early Miocene, that are suggested by such alteration cycles in SE Asia, may have controlled cyclic terrestrial nutrient supplies and upwelling currents in the Andaman sea. As a result, periods of strong upwelling activity and/or high terrestrial nutrient inputs may have favored the development of oligophotic and meso-eutrophic, suspension feeders-dominated carbonate factory on top of the Yadana platform, whereas oligo-mesophotic and oligotrophic carbonate factories dominate during periods of lower monsoonal intensity.

Additionally, the Andaman Sea has been extensively studied for the occurrence of high amplitude (>60m) internal solitons (Alpers *et al.,* 1997; Hyder *et al.,* 2005; Jantzen *et al.*, 2013; Osborne & Burch, 1980) Locally, solitons are related to the occurrence of strong tidal currents in a stratified water column flowing over reliefs inducing abrupt changes in bathymetry, especially, over the sea–mounts from the Andaman volcanic arc (Hyder *et al.,* 2005). Solitons induce perturbations of the depth of the pycnocline and generate strong currents (Apel *et al.,* 1985). In the northern Andaman sea, internal solitons have been shown to displace the pycnocline from an average depth of 30m, down to ~120m (Hyder *et al.*, 2005). Such phenomena probably also occurred during the early Miocene, at a time when the topographic sill of the Andaman Arc was already formed. They may have contributed to enrich shallow-waters in nutrient by mixing with upwelled deeper waters.

Solitons may also be responsible for the episodic high-energy events revealed by the sedimentological analysis of cores.

The balance between rates of sea level changes and sediment accumulation may be potentially responsible for the transition between mesophotic and oligophotic facies since it has controled water depth on top of the platform. During periods of relative oligotrophy, upward transitions from LF1 or LF2.1facies reflecting a mesophotic environment to LF2.2 facies reflecting a oligophotic environment, as observed within units O4 (seismic reflector H9B on Fig. 12) and O6 can be related to a rise in relative sea level that is not compensated by sediment infilling. Moreover, an upward transition from LF1 facies reflecting a mesophotic and oligotrophic environment to LF3.1 or LF3.2 facies typical of oligophotic and meso-eutrophic environment can result from: 1) an increase in nutrient content coupled with an increase in water-depth resulting of positive balance between rate of sea level rise and sediment accumulation, 2) an increase in nutrient content alone accompanied by a decrease in water transparency, without bathymetric changes. As a consequence, changes in trophic level over time make difficult to decipher palaeobathymetric trends and amplitude to assess the relative-sea-level control on the composition of UBL carbonates.

Subsidence is, together with eustacy, the parameter governing changes in accommodation thus governing the deposition of thick (up to 850m), shallow-water carbonates on the Yadana shelf (Paumard *et al.*, 2017). Considering the relatively low subsidence rates calculated from the Oligocene to Miocene carbonates from the Yadana platform (~30 m / Myr; LBL + UBL, Fig. 4B), eustatic changes probably largely controlled the third-order (0.5 – 5 Myr) variations in relative sea-level. The maximum amplitude of eustatic sea-level changes during the Early Miocene is ~40 metres (Fig. 4B) after Miller *et al.* (2005). Such variations would be consistent with the mesophotic-oligophotic transitions evidenced in the oligotrophic intervals from Yadana.

The significance of oligo-mesophotic carbonate factories in the Cenozoic of SE Asia

The concept of 'tropical carbonate factory', that is defines a carbonate production dominated by photosynthetic autotrophs (e.g. green algae) and organisms with photosynthetic symbionts (e.g. zooxanthellate corals and LBF) living in warm, shallow-water, well-illuminated, oligotrophic, has been extensively used to typify carbonate paleoenvironments in various Cenozoic sub-tropical to tropical area (Hallock & Glenn, 1986; Schlager, 2000; Schlager, 2003). Nevertheless, an important number of recent studies in the Mediterranean region (e.g. Morsilli *et al.* 2012; Pomar *et al.* 2014, 2017) have increasingly identified facies associations and geometries significantly different from the "standard" modern tropical carbonate model based on reef systems and stressing the importance of the meso-oligophotic carbonate production by larger benthic foraminifers (LBF), red algae, associated to scleractinians. Similarly, the role of mesophotic carbonate factories in Oligo-Miocene carbonate systems has been also evidenced in the Perla field (offshore Venezuela, Carribean domain), where most carbonate sediments have been shown to be produced in the deeper part of the photic zone (Pomar, 2015).

In tropical, Cenozoic to modern environments from SE Asia, heterozoan carbonate production has been shown to be significant and sometimes dominant in area where upwelling and/or terrestrial runoff, high turbidity and cool waters occur (Halfar & Mutti, 2005; Madden & Wilson, 2013; Wilson & Vecsei, 2005). In such environments, heterotrophic and mixotrophic biota commonly outweighs photosynthetic autotrophs (Tomascik *et al.*, 2000; Wilson & Vecsei, 2005). Under conditions of high nutrient supply and high water turbidity, large scale, isolated and land-attached oligophotic platforms are developing in modern environments (Paternoster platform: *Burollet et al.* 1986 ; Spermonde platform: Renema and Troelstra 2001 ; Kalukalukung banks: Roberts &

Phipps 1988, Saya de Malha Bank: Hilbertz & Goreau 2002). Cenozoic counterparts have been also described: Berai platform (Saller & Vijaya, 2002); Tonasa platform (Wilson & Bosence, 1996) ; and Melinau platforms (Adams, 1965). In these carbonate systems, the oligophotic carbonate production dominates while a euphotic carbonate production may occur in some shallow-waters areas (Wilson & Vecsei, 2005), including barrier reefs or shoal rims (e.g. Paternoster and Berai Platforms), or localized patch/pinnacle reefs (e.g. Spermonde shelf). Shallow area with euphotic carbonate production may be of very reduced extensions in some banks or incipiently drowned platforms such as in the Wonosari and Kalukalukuangs platforms (Read, 1985). The present study shows, that isolated carbonate systems with exclusive oligo-mesophotic carbonate production existed during the Early Miocene in Southeast Asia and that "incipiently drowned platform" conditions persisted throughout the entire Early Miocene interval. On the Yadana platform, oligo-mesophotic carbonate production has been persistent during the Early Miocene and has been promoted by the combination of repeated periods of high nutrient supply from terrestrial runoff (Irrawaddy River), upwelling currents related to monsoonal activity and deep-water mixing controlled by internal waves.

The main striking features of the Yadana platform is the development of coral-rich limestones in oligo-mesophotic environments in contrast to most other Oligo-Miocene carbonate systems from SE Asia (Wilson, 2002 and references therein), where scleractinian-dominated carbonate production is generally related to euphotic conditions, even in nutrient-rich and/or siliciclastic-rich environments (Wilson, 2005; Wilson & Vecsei, 2005). In the Mediterranean regions (Late Eocene, Spain: Morsilli *et al*., 2012 ; Oligocene, Italy: Pomar *et al.,* 2014 ; Miocene, Malta: Baldassini & Di Stefano, 2017), coral bioherms have been shown to develop in oligo-mesophotic environments in high nutrient and high terrigenous supply settings. Such carbonate factories can be considered

as analogues for the Yadana scleractinian-echinodermal carbonate factory that dominates during periods of meso-eutrophy.

Carbonate production dominated by non-framework building biota has been evidenced in Oligo-Miocene, euphotic environments from the Indo-Pacific realm. Probably, the most significant non-framework building euphotic carbonate factory relates to foraminiferal and coralline algal and scleractinian production in sea-grass environments. Isolated carbonate buildups with dominant sea-grass-related carbonate production has been in the Late Oligocene and Early Miocene from the Malampaya buildup, Philippines, where changes in trophic states have operated *(*Fournier *et al.,* 2004). The Malampaya and Yadana isolated systems show a number of similarities, including their predominantly aggrading stratigraphic architecture, the flat-topped morphology of the platform and the relative abundance of coral-rich facies. However, they differ mainly in two points: 1) apart from corals, in Malampaya, carbonate production is characterized by seagrass-inhabiting benthic foraminifera (*Austrotrillina*, soritids, alveolinids, *Neorotalia*, *Miogypsina* and *Miogypsinoides*) whereas in Yadana the large foraminifers (lepidocyclinids, *Spiroclypeus*) and encrusting coralline algae are predominant; 2) sedimentation was cyclic in Malampaya as shown by succession of metre-scale parasequences and punctuated by repeated subaerial exposure surfaces. By contrast, at the Yadana site, there are alternations of metre-to-decametre thick, coral-rich and foraminiferal-coralline algal units and hard-grounds are the only remarkable surfaces. Euphotic carbonate production dominated by seagrass dwellers has been also recognized in the Aquitanian and Burdigalian ramps from Nepoui, New Caledonia *(Maurizot et al.,* 2016), and from the Middle-to-Late Miocene Marion Plateau open platform (Conesa *et al.,* 2005) .

Accordingly the finding from the Yadana platform provide new insights into tropical carbonate production in SE Asia during the Cenozoic. Along with the classical euphotic, oligotrophic

carbonate factory (Photozoan *sensu* James 1997), dominated by photosynthetic autotrophs and symbiont-bearing organisms including framework-building corals and LBF (e.g. Wilson & Evans, 2002; Saqab & Bourget, 2016), three significant tropical carbonate factories coexisted in SE Asia during the Miocene: 1) Seagrass-related, euphotic factory, 2) Oligo-mesophotic and oligotrophic LBF and coralline algal factory, and 3) Oligo-mesophotic, meso-eutrophic factory dominated by corals and various suspension-feeders including ophiuroids.

CONCLUSION

Based on a detailed study of biological and sedimentological attributes from cores, well-correlations and seismic expression, a revised depositional model of the Upper Burma Limestone (UBL) from the Yadana platform is proposed and interpreted in terms of changes in turbidity, light penetration, hydrodynamic water energy and nutrient availability.

1) The layer-caked architecture inferred from seismic and well-correlations, together with the low lateral changes in lithofacies suggest a deposition on top of a flat-topped and open platform throughout the Early Miocene interval. Oligo-mesophotic biological associations dominate whereas strictly euphotic constituents testifying to the proximity of typical reefs or seagrass-related biota are entirely lacking. Three types of carbonate factory operated at the top of the platform, depending on the paleoenvironmental context: 1) a scleractinian-echinodermal factory developing under oligo-mesophotic, and high-nutrient (mesotrophic to eutrophic) conditions, 2) a LBF-coralline algal factory prevailing under mesophotic and

oligotrophic conditions and 3) a LBF factory dominating in oligophotic and oligotrophic settings.

2) The three fundamental parameters controlling carbonate production on the Yadana platform were: 1) light intensity, 2) nutrient content and 3) water energy. The dominantly low-energy setting of the oligo-mesophotic deposits suggests that deposition occurred below the fair-weather wave base. Changes from mesophotic to oligophotic carbonate factories on the Yadana platform top through time may be related either to a change in water depth, or to a change in water transparency. The, occurrence of thin-beds of foraminiferal rudstones, the usual fragmentation of branching rhodoliths and the occurrence of brecciated intervals at top of early cemented coral-echinodermal facies is regarded as indicative of frequent episodic high energy events as storm and/or internal waves.

3) Finally, for the first time in the Oligo-Miocene from SE Asia, the present case study documents the development history of a strictly oligo-mesophotic isolated carbonate platform with significant development of coral-rich deposits. Changes in monsoonal intensity and terrestrial runoff from the river Irrawaddy are thought to have largely controlled the paleoceanographic history of the Andaman Sea during the Early Miocene. These events were likely responsible for the repeated development of high-nutrient, low-to-moderate water transparency conditions as well as for the episodic occurrence of upwelling currents and/or internal waves. Such paleoceanographic conditions, characterized by variable trophic regimes, promoted the development of an incipiently

drowned platform, in oligo-mesophotic settings, during the whole Early Miocene time interval.

Table 1. Lithofacies classification and paleoenvironmental interpretations of the UBL formation, based on the main skeletal components and sedimentological attributes.

Fig. 1. Paleogeography of the Andaman Sea and environmental setting of the Yadana field**.** (A) Paleogeography of the Andaman Sea during the Late Oligocene (A) and to the Early Miocene (B) (modified from Licht *et al.,* 2016 ; Morley, 2017). (C) Location map of the Yadana field and tectonic setting of the Andaman Sea (after Curray 2005).

Fig. 2. Morphological and geophysical frame of the Yadana field (A) Depth map of TOP UBL surface interpreted from 2D seismic data showing the Yadana high, the M5 and the Moattama basins. The red square represents the 3D seismic survey of the Yadana field and the red line refers to the seismic profile (Fig. 2C). (B) 3D Seismic survey of the Yadana field, depth map of TOP UBL surface and well location. (C) Interpreted regional 2D seismic profile through the Yadana high (see location on A).

Fig. 3. Structure and stratigraphy of the UBL (A) Interpreted 3D seismic profile (location of the Fig. 2.B.) of the Yadana field passing across the wells YAD-4 and YAD-2 .The lithostratigraphic units and the gas water contact (red dotted line) are showed (B). Lithostratigraphic column of the Yadana platform, name and age of the sedimentary units.

Fig. 4. Chronostratigraphic framework of the Yadana carbonate buildup (A) based on planktonic and large benthic foraminiferal identification from the studied cores (UBL) and side wall cores (LBL & UBL). This work is based on the first appearance of planktonic foraminiferal and shallow benthic foraminiferal zones according to the "letter stages" after BouDagher-Fadel (2008) and BouDagher-Fadel (2015) and relative to the biostratigraphical time scale as defined by Gradstein *et al.* (2012). (B) Chronostratigraphic framework of the Yadana field in relation to eustasy and global climatic events (Miller *et al.*, 2005). (1) Climatic events of the Oligocene-Early Miocene are based on; (1) Miocene Climatic optimum (Holbourn *et al.*, 2005), (2) Proto-monsoon and intensity of South Asian Monsoon SAM (Betzler *et al.*, 2016).

Fig. 5. Microphotographs of **key** large benthic foraminifera of the UBL formation. (A) YAD-2 1354, 95 Assemblage of *Miogypsinella ubaghsi* (Tan Sin Hok, 1936). (B) YAD-3 1350, 24 *Miogypsina intermedia* (Drooger, 1952); (C) YAD-1 1254, 3 *Miogypsinoides bantamensis* (Tan Sin Hok, 1936). (D) YAD-2 1329, 22 *Globigerinoides primordius* (Blow and Banner, 1962), E) YAD-1 1243, 88 a - *Spiroclypeus tidoenganensis* (Van der Vlerk, 1925); b – *Miogypsina subiensis* (BouDagher-Fadel and Price, 2013). (F) YAD-1 1259, 50 *L. (Nephrolepidina) sumatrensis* (Brady, 1875)

Fig. 6. Close-ups of the lithofacies identified in the cores from coralline algal floatstone to rudstone (LF1) and LBF rudstone (LF2.1): (A) YAD-3 1321.97 Coralline algal rudstone (LF1). Encrusting (rhodolith) and warty forms, possible *Lithothamnion* **(Lith)** with small conceptacles. (B) YAD-1 1251.25: Coralline algal floatstone (LF1). Branching *Lithothamnion* **(Lith)** with flat (and refilled)

conceptacles. *L. ramossissimum* type. (C) YAD-3 1323.40: Coralline algal floatstone (LF1) with a foraminiferal-red algal grainstone matrix. Encrusting and branching *Lithothamnion* **(Lith)** with flat conceptacles, *Lt. ramossissimum* type, (D) YAD-2 1262.68: Coralline algal floatstone (LF1). Abundant protuberant crusts of *Sporolithon* **(Sporo)**, (E) YAD-3 1334.48: Coralline algal floatstone (LF1) with a foraminiferal grainstone matrix (LF1). Branching and encrusting forms of coralline algae **(RA)** associated with *Miogypsinoides* **(Miog)**. (F) YAD-3 1340.90: Coralline algal with large benthic foraminiferal floatstone-wackestone (LF2.2). Laminar, loose *Mesophyllum* **(Meso)**. (G) YAD-2 1345: Core picture of rhodolothic rudstone. Rudstone. Black bar length = 7 mm. (G)

Fig. 7. Close-ups of the lithofacies identified in the cores from LBF rudstone (LF2.1) and LBF floatstone (LF2.2) (A) YAD-1 1319.49 Large benthic foraminiferal rudstone (LF2.1) with broken specimens of *Spiroclypeus* and *Lepidocyclinids (Lepidocyclina spp).* Space between bioclasts is filled by calcitic cements. (B) YAD-2 1291.8 Oriented core sample of lithofacies LF2.1. (C) YAD-1 1270.70 large benthic foraminiferal floatstone (LF2.2) with flat *Spiroclypeus* **(Spiro)**, laminar coralline algae **(RA)** and small pieces of corals **(Coral)**. (D) YAD-3 1344.98 Large benthic foraminiferal floatstone (LF2.2) with flat-shaped *Cycloclypeus* **(Cyclo)**, *Spiroclypeus* **(Spiro)** and laminar coralline algae **(RA)**.

Fig. 8. Close-ups of the lithofacies identified in the cores from coral floatstone (LF3.1) and echinodermal wackestone (LF3.2) (A) YAD-1294.98 leached corals **(Coral)** filled with lime mud (faint ghost texture) set in fine bioclastic wackestone matrix with rare flat large benthic foraminifers **(LBF)** and echinoderms **(Echi)**. (B) YAD-2 1361.42 Cemented coral fragment in a

wackestone-packestone bioclastic matrix dominated by echinoderm fragments (C) YAD-1 1294.7 leached coral in echinodermal wackestone. (D) YAD-4 1258.03 Section of ophiuroids with two stages of light extinction **(1)**. (E) YAD-3 1311.84 Dissolved coral (LF3.1) filled with fine bioclastic micritic matrix (F) YAD-4 1326.22 Bioclastic packestone-wackestone with fragments of echinoderms **(Echi)** (LF3.2).

Fig.9. Close-ups of the lithofacies identified in the cores from (A) YAD-1 1256.6 core sample showing a brecciated coral floatstone with lithophage perforations. (D) YAD-4 1299.2 core sample showing a brecciated coral floatstone (LF3.1) dominated with leached coral fragments. The sediment between intraclasts consists of lime mud. (C) YAD-1 1326.7. Angular intraclasts of LBF (*Spiroclypeus*, *Lepidocyclinds*) rudstone (LF2.1) in echinodermal **(Echi)** wackestone. (D) YAD-4 1269.2. Pseudo-breccia with heterometric touching (low transportation) intraclasts of LF3.1 in fine grey micritic matrix. (E) YAD-3 1295.5 Brecciated surface. Below, LF3.1 floatstone with dissolved coral **(D.Coral).** Above, floatstone-rudstone with LBF and coralline (LF2.1).

Fig. 10. Description of core lithology and environmental interpretations: YAD-2 (A) and YAD-3 (C). Hand specimens from (B) YAD-2 1288 and (D) YAD-3 1308 showing surface microstructural features.

Fig. 11. Description of core lithology and environmental interpretations: YAD-1 (A) and YAD-4 (B).

Fig. 12. Well-correlations and stratigraphic architecture of the Yadana platform, based on LBF biostratigraphy, well-to seismic tie (vertical resolution ~10m) and correlation of lithofacies associations.

Fig. 13. Seismic geometries of the Yadana platform. The location of seismic profiles are indicated on Fig. 13F (red lines). (A) SE-NW-oriented flatten profile, passing through wells YAD-3 and YAD-4 and illustrating the main reflectors crossing wells inside de carbonate platform. (B)SE-NW-orientated profile, passing through wells YAD-3 and YAD-4 and illustrating the continuity and flatness of the reflectors inside the platform. (C) N-S-oriented profile, through well YAD-2 showing the northern and the southern platform margins. The linear and continuous reflectors are sharply truncated below the TOP UBL reflector. (D) E-W-oriented profile, through YAD-4 and YAD-2. See the parallel arrangement of the reflection lines inside the platform. The gas water contact is identifiable on this line. (E) Depth map and coherency map (F) of the TOP UBL showing the uneven and rough topography of TOP UBL reflector, with small sized and rounded depressions (sinkholes?). These could be related to a post-depositional phase of subaerial exposure. The northern, southern and western flanks display various cliffs and terraces that may be interpreted as wave-cut platforms and sea-cliffs.

Fig. 14. Depositional model for the UBL formation: a flat topped oligo-mesophotic buildup. For each depositional stages; **(Left)** facies map of the platform showing the location of well sites. **(Center)** Reconstructed depositional profiles in the hypothesis of no turbid waters**. (Right)** Vertical qualitative trends in nutrient and water-energy and light levels within the water column. The light-intensity zonation with depth is based on the proportion of surface light for different extinction coefficients of light (modified from Morsilli et al. 2012). Lower limit of the euphotic, mesophotic and oligophotic zones depends on

water transparency: deeper in blue (oligotrophic) waters and shallower in green (eutrophic) waters. Curves of light penetration for different extinction coefficients of light are based on Hallock & Schlager, (1986); Kahng et al., (2010).

Adams, C. G. (1965). The Foraminifera and stratigraphy of the Melinau Limestone, Sarawak, and its importance in Tertiary correlation. *Quarterly Journal of the Geological Society*, ***121*(1–4)**, 283–338.

Adams, C. G. (1970). A reconsideration of the East Indian Letter Classification of the Tertiary. *Bulletins of the British Museum (Natural History)*, ***19*(3)**, 87–137. Retrieved from http://biostor.org/reference/118699

Adey WH. (1979). Crustose coralline algae as microenvironmental indicators in the tertiary. In : Gar J, Boucot (eds) Historiacal biogeographyn plate tectonics and the chnaging environment. *Oregon State University Press, Corvallis*, 459–464.

Alamaru, A., Loya, Y., Brokovich, E., Yam, R., and Shemesh, A. (2009). Carbon and nitrogen utilization in two species of Red Sea corals along a depth gradient: Insights from stable isotope analysis of total organic material and lipids. *Geochimica et Cosmochimica Acta*, ***73*(18)**, 5333–5342.

Alpers, W., Wang-Chen, H., and Hock, L. (1997). Observation of internal waves in the Andaman Sea by ERS SAR. *European Space Agency, (Special Publication) ESA SP*, **(414 PART 3)**, 1287–1291.

Anderson, G. C. (1969). Subsurface Chlorophyll Maximum in the Northeast Pacific Ocean. *Limnology and Oceanography*, ***14*(3)**, 386–391.

Apel, J. R., Holbrook, J. R., Liu, A. K., and Tsai, J. J. (1985). The Sulu Sea Internal Soliton Experiment. *Journal of Physical Oceanography*.

Aronson, R. B. (2009). Metaphor, inference, and prediction in paleoecology: climate change and the Antarctic bottom fauna. *The Paleontological Society Papers*, ***15***, 177–194.

Aronson, R. B., Blake, D. B., and Oji, T. (1997). Retrograde community structure in the late

Eocene of Antarctica Retrograde community structure in the late Eocene of Antarctica — Geology. *Geology*, ***25*(10)**, 903–906.

Atkinson, M. J., and Bilger, R. W. (1992). Effects of water velocity on phosphate uptake in coral reef-flat communities. *Limnol. Oceanogr.*, ***37*(2)**, 273–279.

Baldassini, N., and Di Stefano, A. (2017). Stratigraphic features of the Maltese Archipelago: a synthesis. *Natural Hazards*, ***86***, 203–231.

Bassi, D. (2005). Larger foraminiferal and coralline algal facies in an Upper Eocene storm-influenced, shallow-water carbonate platform (Colli Berici, north-eastern Italy). *Palaeogeography, Palaeoclimatology, Palaeoecology*, ***226*(1–2)**, 17–35.

Bassi, D., Hottinger, L., and Nebelsick, J. H. (2007). Larger foraminifera from the upper Oligocene of the Venetian area, north-east Italy. *Palaeontology*, ***50*(4)**, 845–868.

Beavington-Penney, S. J., and Racey, A. (2004). Ecology of extant nummulitids and other larger benthic foraminifera: Applications in palaeoenvironmental analysis. *Earth-Science Reviews*, ***67*(3–4)**, 219–265.

Berggren, W. A., Kent, D. V., Swisher, C. C., and Aubry, M.-P. (1995). *a Revised Cenozoic Geochronology and Chronostratigraphy*. *Geochronology, Time Scales, and Global Stratigraphic Correlation*.

Betzler, C, Eberli, G. P., Kroon, D., Wright, James D., Swart, P. K., Nath, B. N., Alvarez-Zarikian, C. A., Alonso-Garciá, M., Bialik, O. M., Blättler, C. L., Guo, J. A., Haffen, S., Horozal, S., Inoue, M., Jovane, L., Lanci, L., Laya, J. C., Mee, A. L. H., Lüdmann, T., Nakakuni, M., Niino, K., Petruny, L. M., Pratiwi, S. D., Reijmer, J. J.G., Reolid, J., Slagle, A. L., Sloss, C. R., Su, X., Yao, Z. and **Young, J. R.** (2016). The abrupt onset of the modern South Asian Monsoon winds. *Scientific Reports*, ***6*(April)**, 1–10.

Betzler, C., Eberli, G. P.,Lüdmann, T., Reolid, J., Kroon, D., Reijmer, J. J.G., Swart, P. K. ,

Wright, J., Young, J. R., Alvarez-Zarikian, C., Alonso-García, M., Bialik, O. M., Blättler, C. L., Guo, J. A., Haffen, S., Horozal, S., Inoue, M., Jovane, L., Lanci, L., Laya, J. C., Hui Mee, A. L., Nakakuni, M., Nath, B. N., Niino, K., Petruny, L. M., Pratiwi, S. D., Slagle, A. L., Sloss, C. R., Su, X., and **Yao, Z..** (2018). Refinement of Miocene sea level and monsoon events from the sedimentary archive of the Maldives (Indian Ocean). *Progress in Earth and Planetary Science*, ***5*(1)**.

Bosence, D. W. J. (1983). Decription and Classification of Rhodoliths (Rhodoids, Rhodolites). *Coated Grains*, **(C)**, 217–224.

Bouchette, F., Séguret, M., and Moussine-Pouchkine, A. (2001). Coarse carbonate breccias as a result of water-wave cyclic loading (uppermost Jurassic - South-East Basin, France). *Sedimentology*, ***48*(4)**, 767–789.

BouDagher-Fadel F. T., M. and B. (1999). Revision of the stratigraphic significance of the Oligocene-Miocene "letter-stages". *Revue de Micropaléontologie*, ***42*(2)**, 93–97.

BouDagher-Fadel, M. K. (2008). *Evolution and geological significance of larger benthic foraminifera*.

BouDagher-Fadel, M. K. (2015). *Biostratigraphic and geological significance of planktonic foraminifera*.

Braga, J. C., and Aguirre, J. (2004). Coralline algae indicate Pleistocene evolution from deep, open platform to outer barrier reef environments in the northern Great Barrier Reef margin. *Coral Reefs*, ***23*(4)**, 547–558.

Braga, J. C., Bassi, D., and Piller, W. (2010). Palaeoenvironmental significance of Oligocene – Miocene coralline red algae – a review, 165–182.

Burollet, P. F., Boichard, R., Lambert, B., and Villain, J. M. (1986). The Pater Noster Carbonate Platform. *AAPG Bulletin*, ***1***, 155–169.

Buxton, M. W. N., and Pedley, H. M. (1989). Short Paper: A standardized model for Tethyan Tertiary carbonate ramps. *Journal of the Geological Society*, ***146*****(5)**, 746–748.

Chakraborty, A., and Ghosh, A. K. (2016). Ocean upwelling and intense monsoonal activity based on late Miocene diatom assemblages from Neil Island, Andaman and Nicobar Islands, India. *Marine Micropaleontology*, ***127***, 26–41.

Chakraborty, P. P., and Khan, P. K. (2009). Cenozoic geodynamic evolution of the Andaman-Sumatra subduction margin: Current understanding. *Island Arc*, ***18*****(1)**, 184–200.

Chan, Y. L., Pochon, X., Fisher, M. A., Wagner, D., Concepcion, G. T., Kahng, S. E., … Gates, R. D. (2009). Generalist dinoflagellate endosymbionts and host genotype diversity detected from mesophotic (67-100 m depths) coral Leptoseris. *BMC Ecology*, ***9***, 1–7.

Chatterjee, A., Shankar, D., McCreary, J. P., Vinayachandran, P. N., and Mukherjee, A. (2017). Dynamics of Andaman Sea circulation and its role in connecting the equatorial Indian Ocean to the Bay of Bengal. *Journal of Geophysical Research: Oceans*, ***122*****(4)**, 3200–3218.

Clift, P. D., Hodges, K. V., Heslop, D., Hannigan, R., Van Long, H., and Calves, G. (2008). Correlation of Himalayan exhumation rates and Asian monsoon intensity. *Nature Geoscience*, ***1*****(12)**, 875–880.

Clift, P. D., and Vanlaningham, S. (2010). A climatic trigger for a major Oligo-Miocene unconformity in the Himalayan foreland basin. *Tectonics*, ***29*****(5)**, 1–18.

Curray, J. R. (2005). Tectonics and history of the Andaman Sea region. *Journal of Asian Earth Sciences*, ***25*****(1)**, 187–232.

Feely, R. A., Sabine, C. L., Hernandez-Ayon, J. M., Ianson, D., and Hales, B. (2008). Evidence for upwelling of corrosive “acidified” water onto the continental shelf. *Science*,

***320*(5882)**, 1490–1492.

Fournier, F., Montaggioni, L., and Borgomano, J. (2004). Paleoenvironments and high-frequency cyclicity from Cenozoic South-East Asian shallow-water carbonates: A case study from the Oligo-Miocene buildups of Malampaya (Offshore Palawan, Philippines). *Marine and Petroleum Geology*, ***21*(1)**, 1–21.

Freiwald, A., and Henrich, R. (1994). Reefal coralline algal build- ups within the Arctic Circle: morphology and sedimentary dynamics under extreme environmental seasonality. *Sedimentology*, ***41*(5)**, 963–984.

Fulthorpe Schlanger. (1989). Paleo-Oceanographic and tectonic settings of early Miocene reefs and associated carbonates of offshore southeast Asia.

Gilles A.R. Conesa, Eric Favre, Philippe Münch, Dalmasso, H., and Christian Chaix. (2005). Biosedimentaty and paleoenvironmental evolution of the southern Marion platform from the Middle to Late Miocene (Northeast Australia, ODP LEG 194, sites 1196 and 1199). *Proceedings of the Ocean Drilling Program*, ***194*(August)**.

Gradstein, F., Ogg, J., Schmitz, M., and Ogg, G. (2012). *The Geologic Time Scale 2012* (Vol. 1).

Halfar, J., and Mutti, M. (2005). Global dominance of coralline red-algal facies: A response to Miocene oceanographic events. *Geology*, ***33*(6)**, 481–484.

Hallock, P., and Glenn, E. C. (1986). Larger Foraminifera: A Tool for Paleoenvironmental Analysis of Cenozoic Carbonate Depositional Facies. *Palaios*, ***1*(1)**, 55–64.

Hallock, P., and Pomar, L. (2012). Cenozoic Evolution of Carbonate Shelf and Ramp Habitats: Insights from Paleoceanography, ***50663*(SEPTEMBER 2014)**.

Hallock, P., Premoli Silva, I., and Boersma, A. (1991). Similarities between planktonic and

larger foraminiferal evolutionary trends through Paleogene paleoceanographic changes. *Palaeogeography, Palaeoclimatology, Palaeoecology*, ***83*****(1–3)**, 49–64.

Hallock, P., and Schlager, W. (1986). Nutrient Excess and the Demise of Coral Reefs and Carbonate Platforms. *Palaios*, ***1*****(4)**, 389.

Haq, B. U., Hardenbol, J., and Vail, P. R. (1987). Chronology of Fluctuating Sea Levels Since the Triassic. *Science*, ***235*****(4793)**, 1156–1167.

Hearn, C., Atkinson, M., and Falter, J. (2001). A physical derivation of nutrient-uptake rates in coral reefs: Effects of roughness and waves. *Coral Reefs*, ***20*****(4)**, 347–356.

Hilbertz, W., and Goreau, T. (2002). Saya de Malha expedition report, **(March)**, 1–107. Retrieved from papers2://publication/uuid/88F1085F-DA19-4918-B17B-DB6C14C96A10

Hine, a. C. (2001). Advances in carbonate sequence stratigraphy: Application to reservoirs, outcrops, and models. *Eos, Transactions American Geophysical Union*, ***82*****(2)**, 18–18.

Holbourn, A., Kuhnt, W., Schulz, M., and Erlenkeuser, H. (2005). Impacts of orbital forcing and atmospheric carbon dioxide on Miocene ice-sheet expansion. *Nature*, ***438*****(7067)**, 483–487.

Hyder, P., Jeans, D. R. G., Cauquil, E., and Nerzic, R. (2005). Observations and predictability of internal solitons in the northern Andaman Sea. *Applied Ocean Research*, ***27*****(1)**, 1–11.

James, N. P. (1997). The cool-water carbonate depositional realm. *Sedimentary Geology*, ***56***, 1–20.

Jantzen, C., Schmidt, G. M., Wild, C., Roder, C., Khokiattiwong, S., and Richter, C. (2013). Benthic reef primary production in response to large amplitude internal waves at the Similan Islands (Andaman Sea, Thailand). *PLoS ONE*, ***8*****(11)**, 1–16.

Kahng, S. E., Garcia-Sais, J. R., Spalding, H. L., Brokovich, E., Wagner, D., Weil, E., Hinderstein, L. and **Toonen, R. J.** (2010). Community ecology of mesophotic coral reef

ecosystems. *Coral Reefs*, ***29*(2)**, 255–275.

Lesser, M. P., Slattery, M., and Leichter, J. J. (2009). Ecology of mesophotic coral reefs. *Journal of Experimental Marine Biology and Ecology*, ***375*(1–2)**, 1–8.

Licht, A., Reisberg, L., France-Lanord, C., Naing Soe, A., and Jaeger, J. J. (2016). Cenozoic evolution of the central Myanmar drainage system: Insights from sediment provenance in the Minbu Sub-Basin. *Basin Research*, ***28*(2)**, 237–251.

Liebau, A. (1984). Grunddlagen der Ökobathymetrie. *Paläontologische*, ***2***, 149–184.

Madden, R. H. C., and Wilson, M. E. J. (2013). Diagenesis of a SE Asian Cenozoic carbonate platform margin and its adjacent basinal deposits. *Sedimentary Geology*, ***286–287***, 20–38.

Mass, T., Einbinder, S., Brokovich, E., Shashar, N., Vago, R., Erez, J., and Dubinsky, Z. (2007). Photoacclimation of Stylophora pistillata to light extremes: Metabolism and calcification. *Marine Ecology Progress Series*, ***334*(June 2014)**, 93–102.

Mateu-Vicens, G., Pomar, L., and Ferràndez-Canadell, C. (2012). Nummulitic banks in the upper Lutetian "Buil level", Ainsa Basin, South Central Pyrenean Zone: The impact of internal waves. *Sedimentology*, ***59*(2)**, 527–552.

Maurizot, P, Cabioch, G., Fournier, F., Leonide, P., Sebih, S., Rouillard, P., Montaggioni, L., Collot, J., Martin-Garin, B., Chaproniere, G., Braga, Juan C. and **Sevin, B.** (2016). Post-obduction carbonate system development in New Caledonia (Népoui, Lower Miocene). *Sedimentary Geology*, ***331***, 42–62.

McKinney, F. K., and Hageman, S. J. (2007). Crossing the Ecological Devide: Paleozoic to Modern Marine Ecosystems in the Adriatic Sea. *The Sedimentary Record*, ***5*(2)**.

Miller, K. G., Kominz, M. A., Browning, J. V., Wright, J. D., Mountain, G. S., Katz, M. E., Sugarman, P. J., Cramer, B. S., Christie-Blick, N. and **Pekar, S. F.** (2005). The phanerozoic record of global sea-level change. *Science*, ***310*(5752)**, 1293–1298.

Morley, C. K. (2017). Chapter 4 Cenozoic rifting, passive margin development and strike-slip faulting in the Andaman Sea: a discussion of established v. new tectonic models. *Geological Society, London, Memoirs*, ***47*(1)**, 27–50.

Morsilli, M., Bosellini, F. R., Pomar, L., Hallock, P., Aurell, M., and Papazzoni, C. A. (2012). Mesophotic coral buildups in a prodelta setting (Late Eocene, southern Pyrenees, Spain): A mixed carbonate-siliciclastic system. *Sedimentology*, ***59*(3)**, 766–794.

Morsilli, M., and Pomar, L. (2012). Internal waves vs. surface storm waves: A review on the origin of hummocky cross-stratification. *Terra Nova*, ***24*(4)**, 273–282.

Muscatine, L., Falkowski, P. G., Dubinsky, Z., Cook, P. A., and McCloskey, L. R. (1989). The Effect of External Nutrient Resources on the Population Dynamics of Zooxanthellae in a Reef Coral. *Proceedings of the Royal Society B: Biological Sciences*, ***236*(1284)**, 311–324.

Noad, J. (2001). The Gomantong Limestone of eastern Borneo: A sedimentological comparison with the near-contemporaneous Luconia Province. *Palaeogeography, Palaeoclimatology, Palaeoecology*, ***175*(1–4)**, 273–302.

Osborne, A. R., and Burch, T. L. (1980). Internal Solitons in the Andaman Sea. *Science*, ***208*(4443)**, 451–460.

Paumard, V., Zuckmeyer, E., Boichard, R., Jorry, S. J., Bourget, J., Borgomano, J. and **Maurin, T.** (2017). Evolution of Late Oligocene - Early Miocene attached and isolated carbonate platforms in a volcanic ridge context (Maldives type), Yadana field, offshore Myanmar. *Marine and Petroleum Geology*, ***81*(March)**, 361–387.

Pomar. (2015). Follow the food; the waxing & waning of coral buildups during the Cenozoic. *Ias Regional Meeting*, 2015.

Pomar, L. (2001). Types of carbonate platforms: A genetic approach. *Basin Research*, ***13*(3)**, 313–334.

Pomar, L., Baceta, J. I., Hallock, P., Mateu-Vicens, G., and Basso, D. (2017). Reef building and carbonate production modes in the west-central Tethys during the Cenozoic. *Marine and Petroleum Geology*, ***83***, 261–304.

Pomar, L., Bassant, P., Brandano, M., Ruchonnet, C., and Janson, X. (2012). Impact of carbonate producing biota on platform architecture: Insights from Miocene examples of the Mediterranean region. *Earth-Science Reviews*, ***113*****(3–4)**, 186–211.

Pomar, L., and Hallock, P. (2008). Carbonate factories: A conundrum in sedimentary geology. *Earth-Science Reviews*, ***87*****(3–4)**, 134–169.

Pomar, L., Martinez, W., Espino, D., Ott, V. C. De, and Benkovics, L. (2015). Oligocene-Miocene Carbonates of the Perla Field, Offshore Venezuela: Depositional Model and Facies Architecture.

Pomar, L., Mateu-Vicens, G., Morsilli, M., and Brandano, M. (2014). Carbonate ramp evolution during the Late Oligocene (Chattian), Salento Peninsula, southern Italy. *Palaeogeography, Palaeoclimatology, Palaeoecology*, ***404*****(JUNE)**, 109–132.

Pomar, L., Morsilli, M., Hallock, P., and Badenas, B. (2011). Internal waves, an under-explored source of turbulence events in the sedimentary record. *Earth-Science Reviews*, ***111*****(1–2)**, 56–81.

Pyle, R. L., Boland, R., Bolick, H, Bowen, B. W., Bradley, C. J., Kane, C., Kosaki, R. K., Langston, R., Longenecker, K., Montgomery, A., Parrish, Fr. A., Popp, B. N., Rooney, John, Smith, Celia M., Wagner, D., Spalding, H. L. (2016). A comprehensive investigation of mesophotic coral ecosystems in the Hawaiian Archipelago. *PeerJ*, ***4***, e2475.

Racey, A. (2015). Petroleum geology of the Moattama Region, Myanmar.

Rahmani, A., Vaziri-Moghaddam, H., Taheri, A., and Ghabeishavi, A. (2009). A model for the paleoenvironmental distribution of larger foraminifera of Oligocene-Miocene carbonate

rocks at Khaviz Anticline, Zagros Basin, SW Iran. *Historical Biology*, ***21*****(3–4)**, 215–227.

Ramaswamy, V., Rao, P. S., Rao, K. H., Thwin, S., Rao, N. S., and Raiker, V. (2004). Tidal influence on suspended sediment distribution and dispersal in the northern Andaman Sea and Gulf of Martaban. *Marine Geology*, ***208*****(1)**, 33–42.

Rao, P. S., Ramaswamy, V., and Thwin, S. (2005). Sediment texture, distribution and transport on the Ayeyarwady continental shelf, Andaman Sea. *Marine Geology*, ***216*****(4)**, 239–247.

Read, J. F. (1985). Carbonate Platforms Facies Model. *AAPG Bulletin*.

Renema, W., and Troelstra, S. R. (2001). Larger foraminifera distribution on a mesotrophic carbonate shelf in SW Sulawesi (Indonesia). *Palaeogeography, Palaeoclimatology, Palaeoecology*, ***175*****(1–4)**, 125–146.

Ribes, M., Coma, R., Atkinson, M. J., and Kinzie, R. A. (2003). Particle removal by coral reef communities: Picoplankton is a major source of nitrogen. *Marine Ecology Progress Series*, ***257*****(August)**, 13–23.

Roberts, H. ., and Phipps, C. V. (1988). Proposed oceanographic controls on modern Indonesian reefs : A turn-off/turn-on mechanism in a monsoonal setting. *Proceedings of the 6th International Coral Reef Symposium, South Sulawesi, Australia*, ***3*****(529–534)**.

Rosler, A., Pretkovi, V., Novak, V., Renema, W., and Braga, J. C. (2015). Coralline Algae From the Miocene Mahakam Delta (East Kalimantan, Southeast Asia). *Palaios*, ***30*****(1)**, 83–93.

Saller, A. (1993). Sequence Stratigraphy of Aggrading and Backstepping Carboante Shelves, Oligocene, Central Kalimantan, Indonesia.

Saller, A. H., and Vijaya, S. (2002). Depositional and diagenetic history of the Kerendan carbonate platform, Oligocene, Central Kalimantan, Indonesia. *Journal of Petroleum*

Geology, ***25*(2)**, 123–150.

Sanders, D. (2003). *Syndepositional dissolution of calcium carbonate in neritic carbonate environments: Geological recognition, processes, potential significance*. *Journal of African Earth Sciences* (Vol. 36).

Saqab, M. M., and Bourget, J. (2016). Seismic geomorphology and evolution of early???mid Miocene isolated carbonate build-ups in the Timor Sea, North West Shelf of Australia. *Marine Geology*, ***379***, 224–245.

Schlager, W. (2000). Sedimentation rates and growth potential of tropical, cool-water and mud-mound carbonate factories,. *Geological Society Special Publication*, ***178***, 217–227.

Schlager, W. (2003). Benthic carbonate factories of the Phanerozoic. *International Journal of Earth Sciences*, ***92*(4)**, 445–464.

Seguret, M., Moussine-Pouchkine, A., Raja Gabaglia, G., and Bouchette, F. (2001). Storm deposits and storm-generated coarse carbonate breccias on a pelagic outer shelf (South-East Basin, France). *Sedimentology*, ***48*(2)**, 231–254.

Steele, J. H., and Yentsch, C. S. (1960). The vertical distribution of chlorophyll. *Journal of the Marine Biological Association of the United Kingdom*, ***39*(2)**, 217–226.

Tomascik, T., Mah, A. J., Nontji, A., and Moosa, M. K. (2000). *The Ecology of the Indonesian Seas. Part I. The Ecology of Indonesia Series, Volume VII* . *The Quarterly Review of Biology* (Vol. 75).

Wade, B. S., Pearson, P. N., Berggren, W. A., and Pälike, H. (2011). Review and revision of Cenozoic tropical planktonic foraminiferal biostratigraphy and calibration to the geomagnetic polarity and astronomical time scale. *Earth-Science Reviews*, ***104*(1–3)**, 111–142.

Wilson, M. E. J. (2002). Cenozoic carbonates in Southeast Asia: Implications for equatorial carbonate development. *Sedimentary Geology*, ***147*****(3–4)**, 295–428.

Wilson, M. E. J. (2005). Development of equatorial delta-front patch reefs during the Neogene, Borneo. *Journal of Sedimentary Research*, ***75*****(1)**, 114–133.

Wilson, M. E. J. (2008). Global and regional influences on equatorial shallow-marine carbonates during the Cenozoic. *Palaeogeography, Palaeoclimatology, Palaeoecology*, ***265*****(3–4)**, 262–274.

Wilson, M. E. J., and Bosence, D. W. J. (1996). The Tertiary evolution of South Sulawesi: a record in redeposited carbonates of the Tonasa Limestone Formation. *Geological Society, London, Special Publications*, ***106*****(1)**, 365–389.

Wilson, M. E. J., and Evans, M. J. (2002). Sedimentology and diagenesis of Tertiary carbonates on the Mangkalihat Peninsula, Borneo: Implications for subsurface reservoir quality. *Marine and Petroleum Geology*, ***19*****(7)**, 873–900.

Wilson, M. E. J., and Hall, R. (2010). Tectonic influences on SE Asian carbonate systems and their reservoir development. *Cenozoic Carbonate Systems of Australasia*, ***SEPM Speci*****(95)**, 13–40.

Wilson, M. E. J., and Vecsei, A. (2005). The apparent paradox of abundant foramol facies in low latitudes: Their environmental significance and effect on platform development. *Earth-Science Reviews*, ***69*****(1–2)**, 133–168.

Figure 1

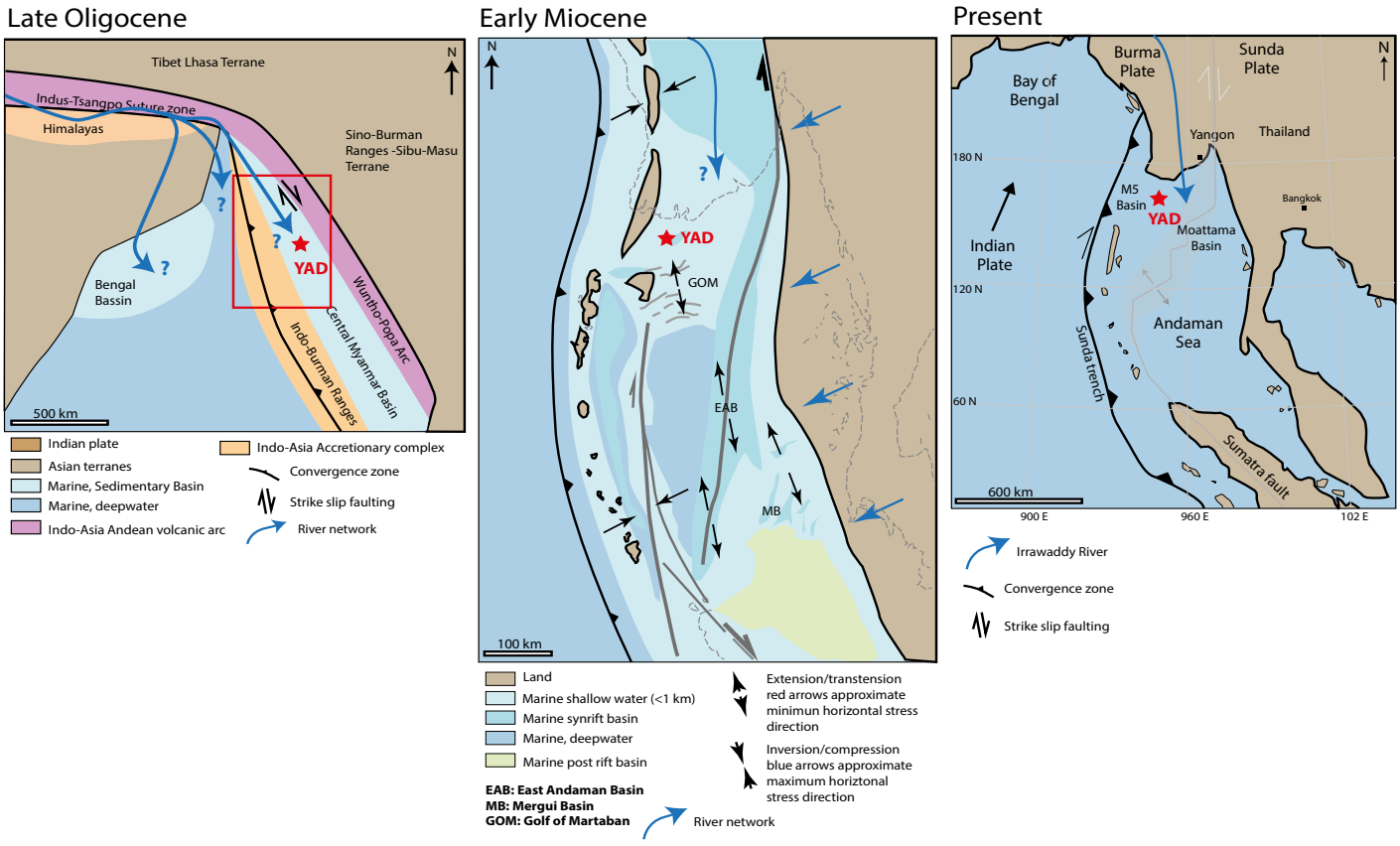
Late Oligocene
Tibet Lhasa Terrane
Indus-Tsangpo Suture zone
Himalayas
Sino-Burman Ranges -Sibu-Masu Terrane
Bengal Bassin
YAD
Wuntho-Popa Arc
Central Myanmar Basin
Indo-Burman Ranges
500 km
N
Indian plate
Asian terranes
Marine, Sedimentary Basin
Marine, deepwater
Indo-Asia Andean volcanic arc
Indo-Asia Accretionary complex
Convergence zone
Strike slip faulting
River network
Early Miocene
YAD
GOM
EAB
MB
100 km
Land
Marine shallow water (<1 km)
Marine synrift basin
Marine, deepwater
Marine post rift basin
EAB: East Andaman Basin
MB: Mergui Basin
GOM: Golf of Martaban
Extension/transtension red arrows approximate minimun horizontal stress direction
Inversion/compression blue arrows approximate maximum horiztonal stress direction
River network
Present
Bay of Bengal
Burma Plate
Sunda Plate
Yangon
Thailand
Bangkok
M5 Basin
YAD
Moattama Basin
Indian Plate
Andaman Sea
Sunda trench
Sumatra fault
180 N
120 N
60 N
600 km
900 E
960 E
102 E
Irrawaddy River
Convergence zone
Strike slip faulting

Figure 2

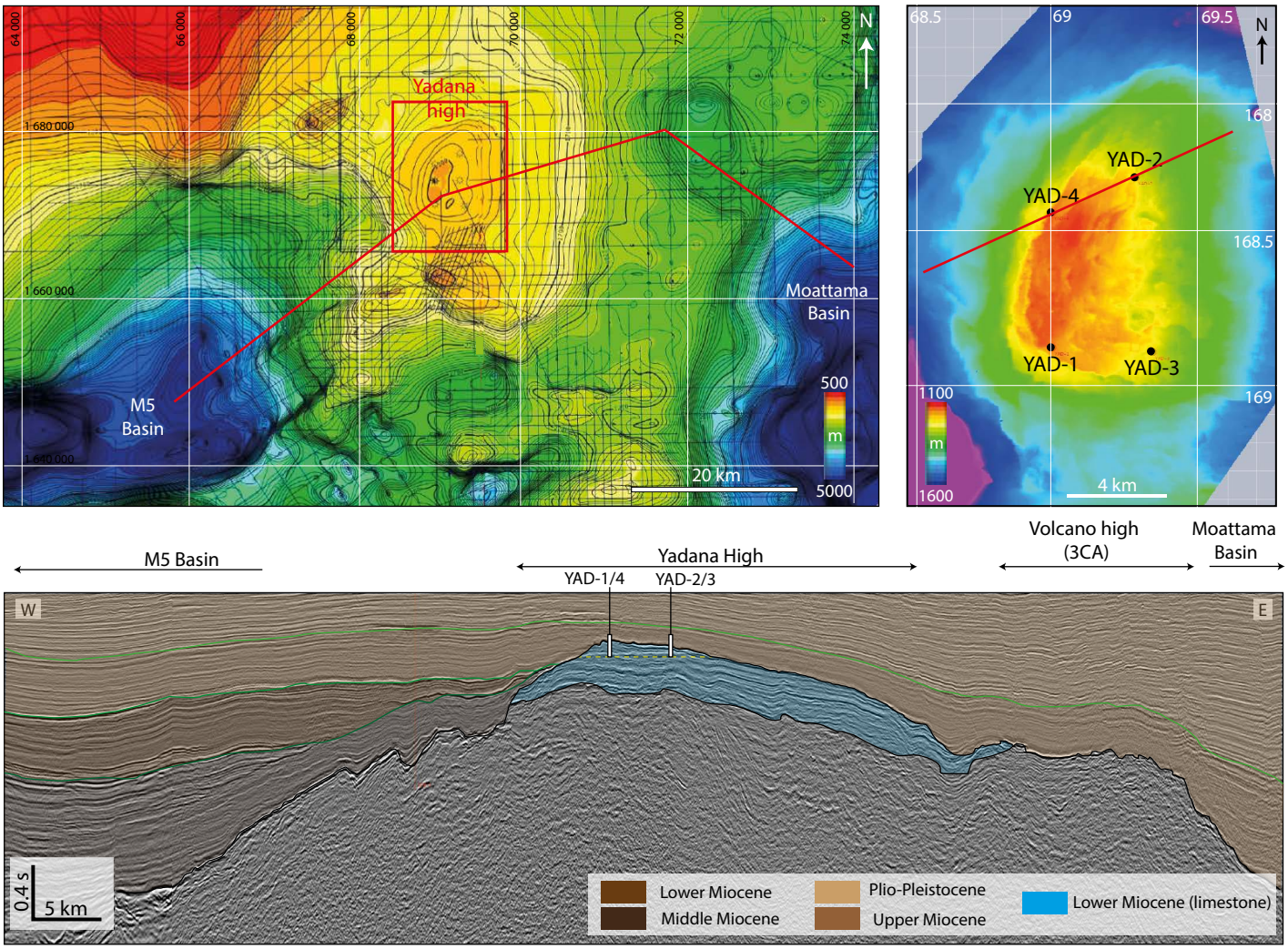
64 000
66 000
68 000
70 000
72 000
74 000
N
1 680 000
1 660 000
1 640 000
Yadana high
M5 Basin
Moattama Basin
500
m
5000
20 km
68.5
69
69.5
N
168
168.5
169
YAD-2
YAD-4
YAD-1
YAD-3
1100
m
1600
4 km
M5 Basin
Yadana High
Volcano high (3CA)
Moattama Basin
YAD-1/4
YAD-2/3
W
E
0.4 s
5 km
Lower Miocene
Middle Miocene
Plio-Pleistocene
Upper Miocene
Lower Miocene (limestone)

Figure 3

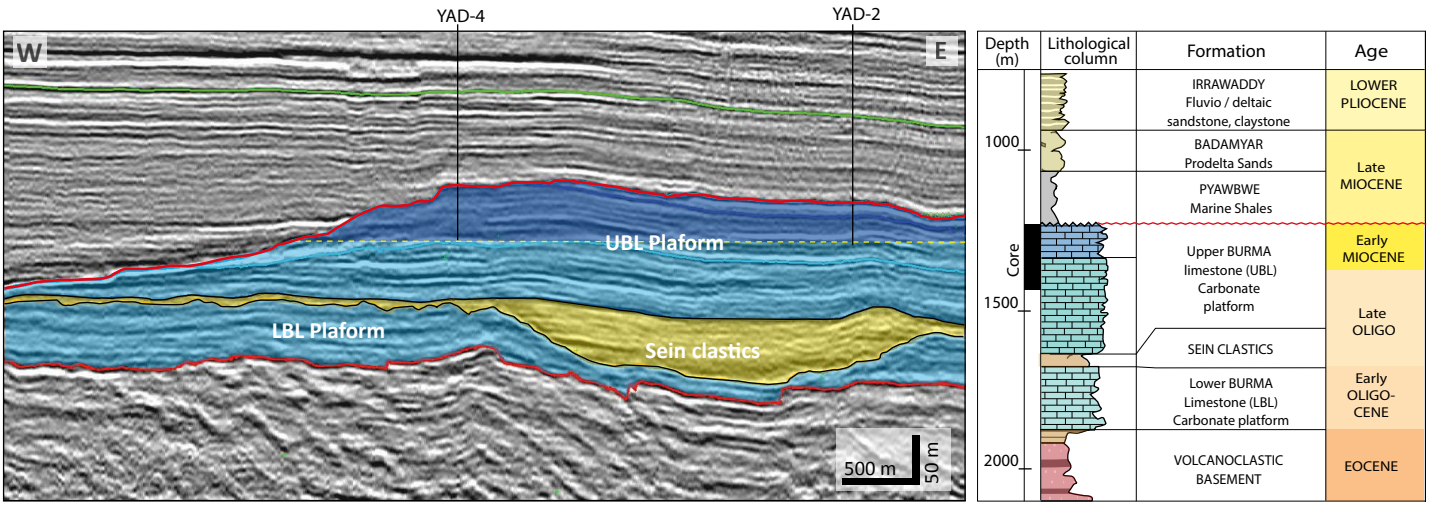
YAD-4
YAD-2
W
E
UBL Plaform
LBL Plaform
Sein clastics
500 m
50 m
Depth (m)
Lithological column
Formation
Age
1000
1500
2000
Core
IRRAWADDY
Fluvio / deltaic sandstone, claystone
LOWER PLIOCENE
BADAMYAR
Prodelta Sands
PYAWBWE
Marine Shales
Late MIOCENE
Early MIOCENE
Upper BURMA limestone (UBL) Carbonate platform
Late OLIGO
SEIN CLASTICS
Lower BURMA Limestone (LBL) Carbonate platform
Early OLIGO-CENE
VOLCANOCLASTIC BASEMENT
EOCENE

Figure 4

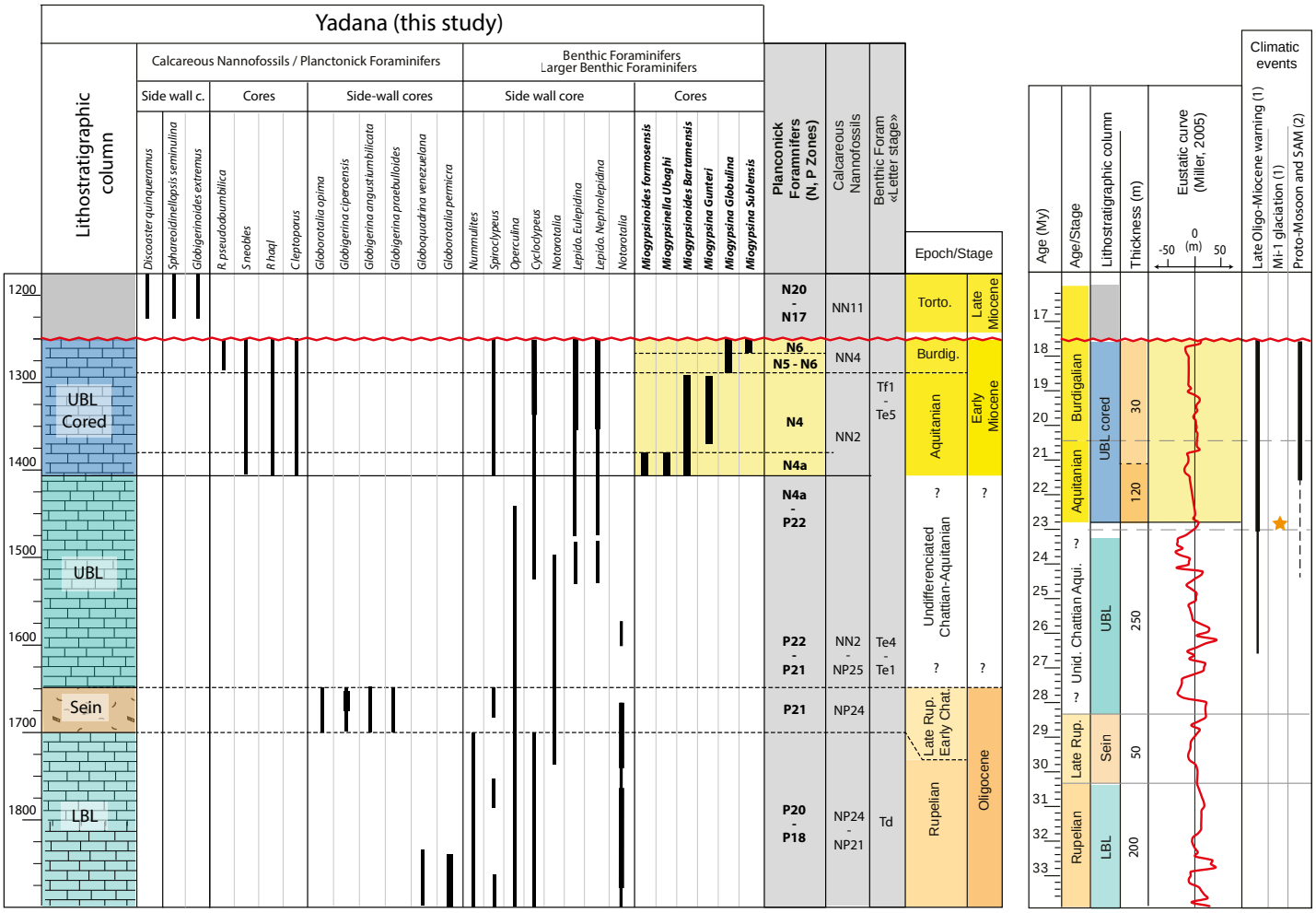
Yadana (this study)
Lithostratigraphic column
Calcareous Nannofossils / Planctonick Foraminifers
Benthic Foraminifers
Larger Benthic Foraminifers
Side wall c.
Cores
Side-wall cores
Side wall core
Cores
Discoaster quinqueramus
Sphaeroidinellopsis seminulina
Globigerinoides extremus
R.pseudodoumbilica
S.neobles
R.haqi
C.leptoporus
Globorotalia apima
Globigerina ciperoensis
Globigerina angustiumbilicata
Globigerina praebulloides
Globoquadrina venezuelana
Globorotalia permicra
Nummulites
Spiroclypeus
Operculina
Cyclodypeus
Notorotalia
Lepida. Eulepidina
Lepida. Nephrolepidina
Notorotalia
Miogypsinoides formosensis
Miogypsinella Uboghi
Miogypsinoides Bantamensis
Miogypsina Gunteri
Miogypsina Globulina
Miogypsina Sublensis
Planconick Foramnifers (N, P Zones)
Calcareous Nannofossils
Benthic Foram «Letter stage»
Epoch/Stage
1200
1300
1400
1500
1600
1700
1800
UBL Cored
UBL
Sein
LBL
N20 - N17
N6
N5 - N6
N4
N4a
N4a - P22
P22 - P21
P21
P20 - P18
NN11
NN4
NN2
NN2 - NP25
NP24
NP24 - NP21
Tf1 - Te5
Te4 - Te1
Td
Torto.
Burdig.
Aquitanian
Undifferenciated Chattian-Aquitanian
Late Rup. Early Chat.
Rupelian
Late Miocene
Early Miocene
Oligocene
Age (My)
Age/Stage
Lithostratigraphic column
Thickness (m)
Eustatic curve (Miller, 2005)
-50
0
50
(m)
Burdigalian
Aquitanian
Unid. Chattian Aqui.
Late Rup.
Rupelian
UBL cored
UBL
Sein
LBL
30
120
250
50
200
Climatic events
Late Oligo-Miocene warning (1)
Mi-1 glaciation (1)
Proto-Mosoon and SAM (2)

Figure 5

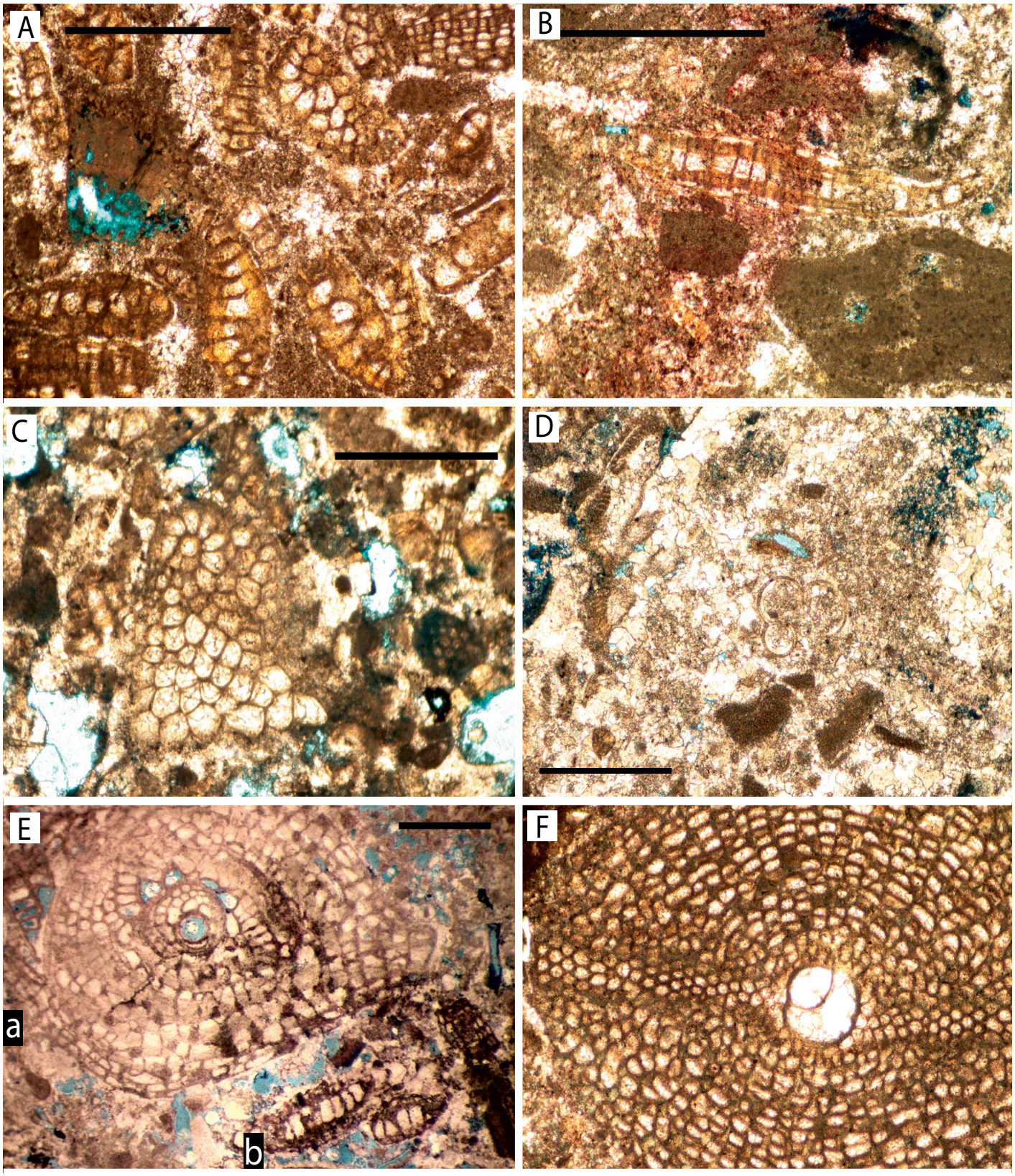

Table 1

Table 1
Lithofacies, skeletal components and interpretation

	Lithofacies	Skeletal components	Interpretation
Coralline algal (LF1)	**LF.1** **Coralline algal floatstone to rudstone** with a coralline algal-foraminiferal wackestone to packestone matrix	Heterometric spheroidal -ellipsoidal rhodoliths (1-10 cm in diameter) or pieces of branching coralline algae (*Lithothamnion, Mesophyllum* and *Sporolithon*). The foraminiferal assemblage is dominated by *Spiroclypeus tidoenganensis* and *Nephrolepidina sumatrensis*, with common occurrences of *Miogypsinoides*, *Miogypsina* and *Heterostegina (Vlerkina)*	Mesophotic zone, oligotrophic (to slightly mesotrophic) conditions, below wave-base, episodic high-energy events. Estimated water-depth: 20-50m.
Large Benthic Foraminiferal dominated (LF2)	**LF2.1** **Large benthic foraminiferal rudstone** with common red algal fragments. Interganular space occupied by peloidal grainstone or occluded by calcite cements	The foraminiferal assemblage is dominated by *Lepidocyclina (Nephrolepidina) sumatrensis, L. (N.) oneatensis*, and *Spiroclypeus tidoenganensis* with rarer specimens of *Amphistegina, Heterostegina, Miogyspina, and Miogypsinoide.* Coralline algae mainly include branching and warty *Lithothamnion*, losse *Mesophyllum* and branching *Sporolithon*	Mesophotic zone, oligotrophic (to slightly mesotrophic) conditions, below wave-base, Deposition during episodic high-energy events. Estimated water-depth: 20-50m.
	LF2.2 **Large benthinc foraminiferal floatstone** with coralline algal wackestone /packestone matrix	Large benthic foraminifers are large (up to 2cm), thin-shelled, commonly well-preserved, and typically horizontally-oriented. Dominated by *Spiroclypeus tidoenganensis* with common occurrences of *Cycloclypeus*... Laminar and loose *Mesophyllum*, together with branching *Lithothaminon* are common	Oligophotic zone, oligotrophic (to slightly mesotrophic) conditions, below wave-base, low energy setting. Estimated water-depth: 50-80m.
Coral floatstone with echinoderm wackestone (LF3)	**LF3.1** **Coral floatstone** embedded in a wackestone matrix dominated by echinoderm. Coral dominated intervals are frequently breciated at the top	Scelaractinian floastone consists of fragile branches or massive fragments of *Faviids* and *Pocilloporids*. Ophiuroids, echinoids, small pieces of non articulated coralline algae and occasional broken *Spiroclypeus* and *lepidocyclinids* Elements of breccias are gravel to pebble-sized (typically 0.5-5 cm), angular, para-autocthonous and does not exhibit evidences of dissolution. The Inter-intraclast space s are filled with a micrite containing various proportions of small echinoderm fragments.	Oligo-mesophotic zone, meso- to eutrophic conditions, below wave-base, episodic high-energy events. Estimated water-depth: 20-50m.
	LF3.2 **Echinodermal wackestone** Bioclastic wackestone	Bioclastic wackestone is dominated by echinoderms pieces including ophiuroid ossicles and echinoids, small size fragments of coralline algae. Frequently interbedded between coral floatstone LF3.1	Oligo-mesohotic zone, meso- to eutrophic conditions, below wave-base, episodic high-energy events. Estimated water-depth: 20-50m.

Figure 6

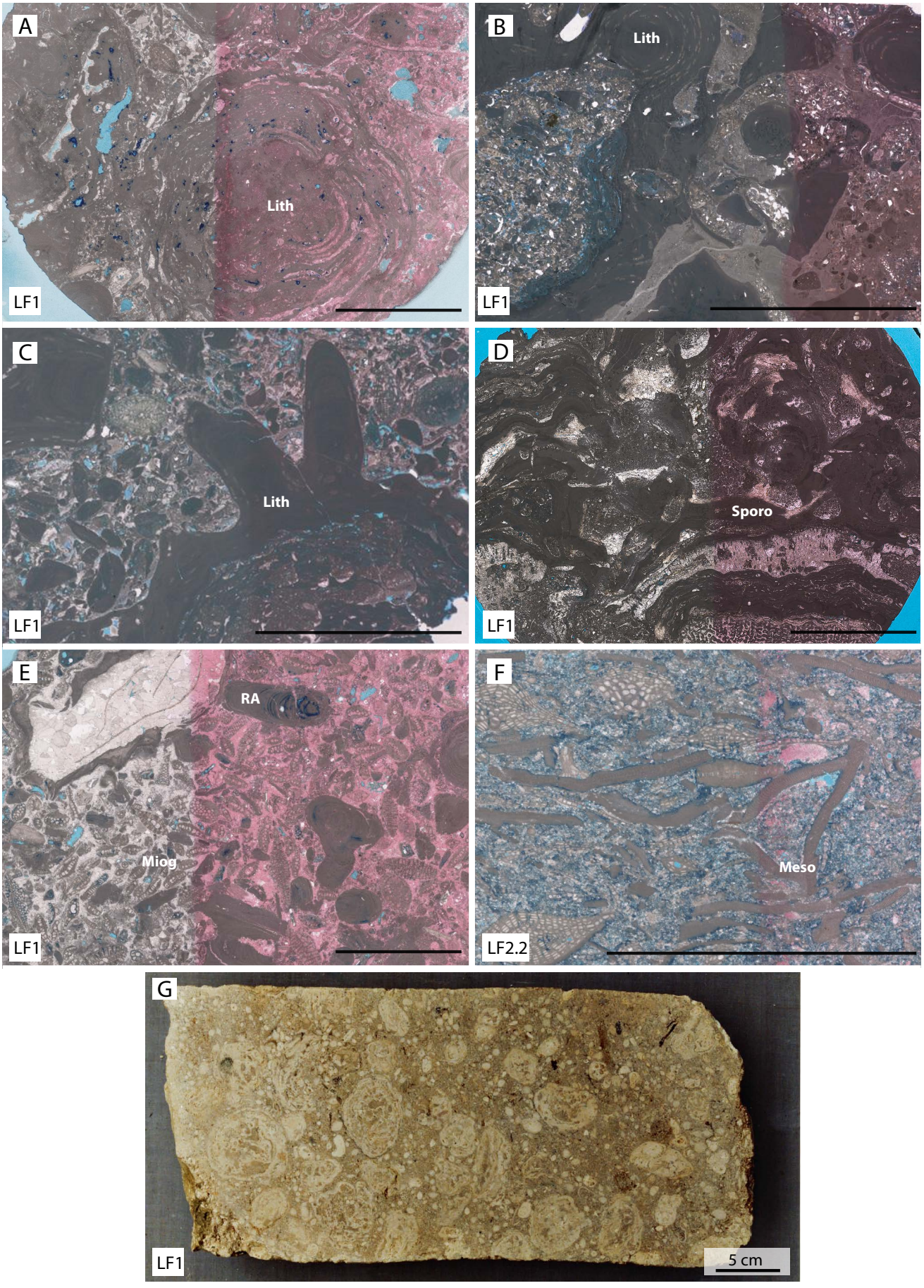
A
Lith
LF1
B
Lith
LF1
C
Lith
LF1
D
Sporo
LF1
E
RA
Miog
LF1
F
Meso
LF2.2
G
LF1
5 cm

Figure 7

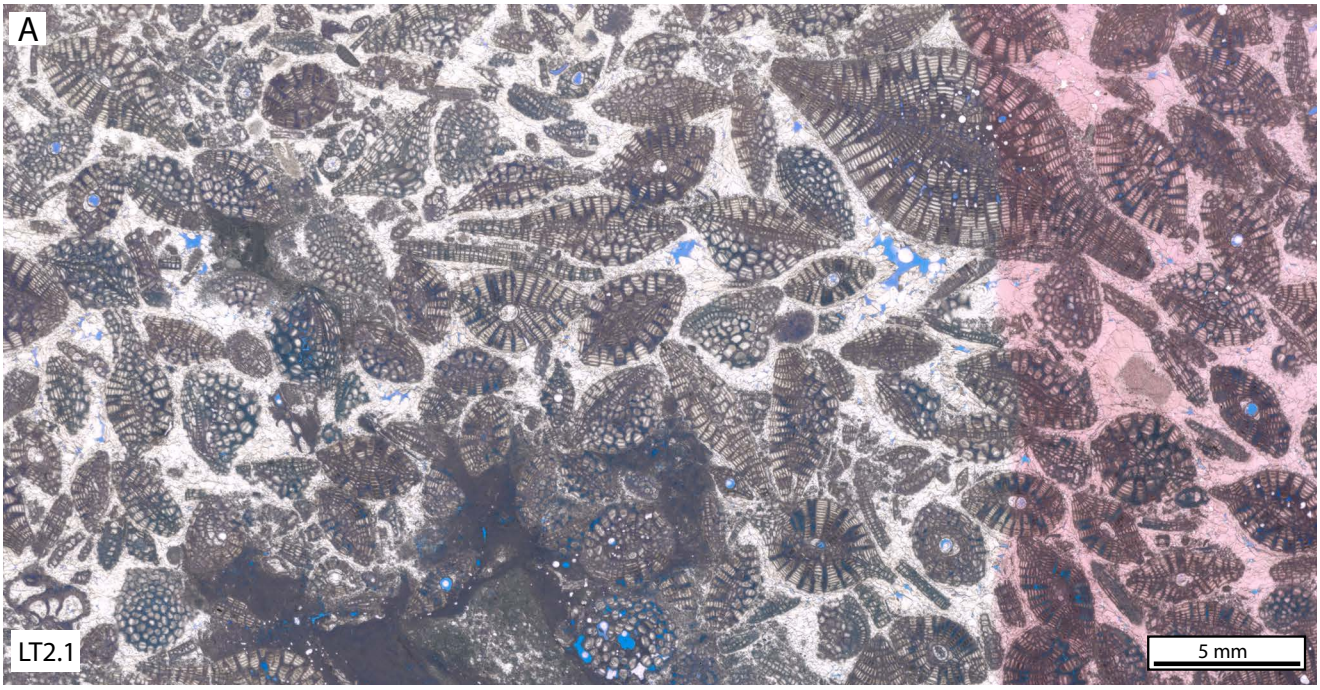
A
LT2.1
5 mm

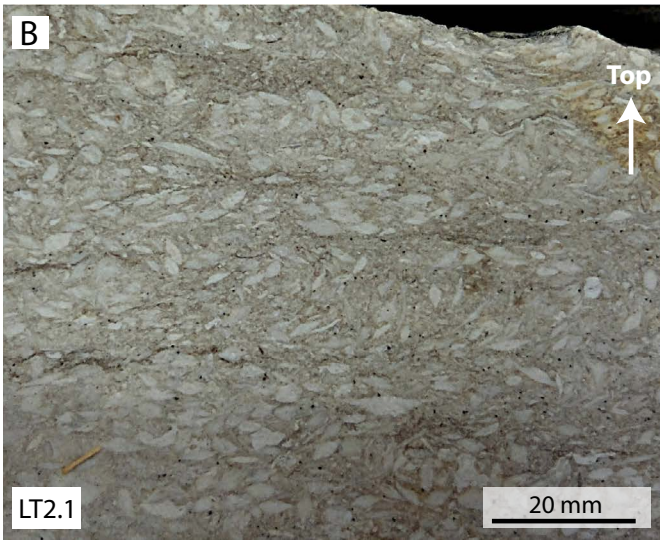
B
Top
LT2.1
20 mm

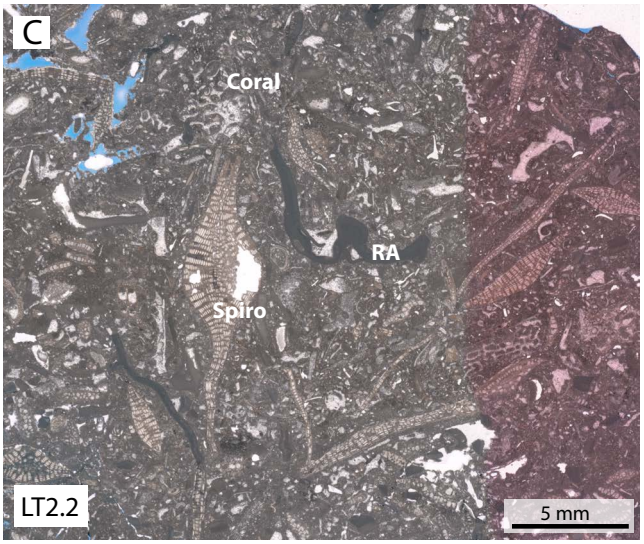
C
Coral
RA
Spiro
LT2.2
5 mm

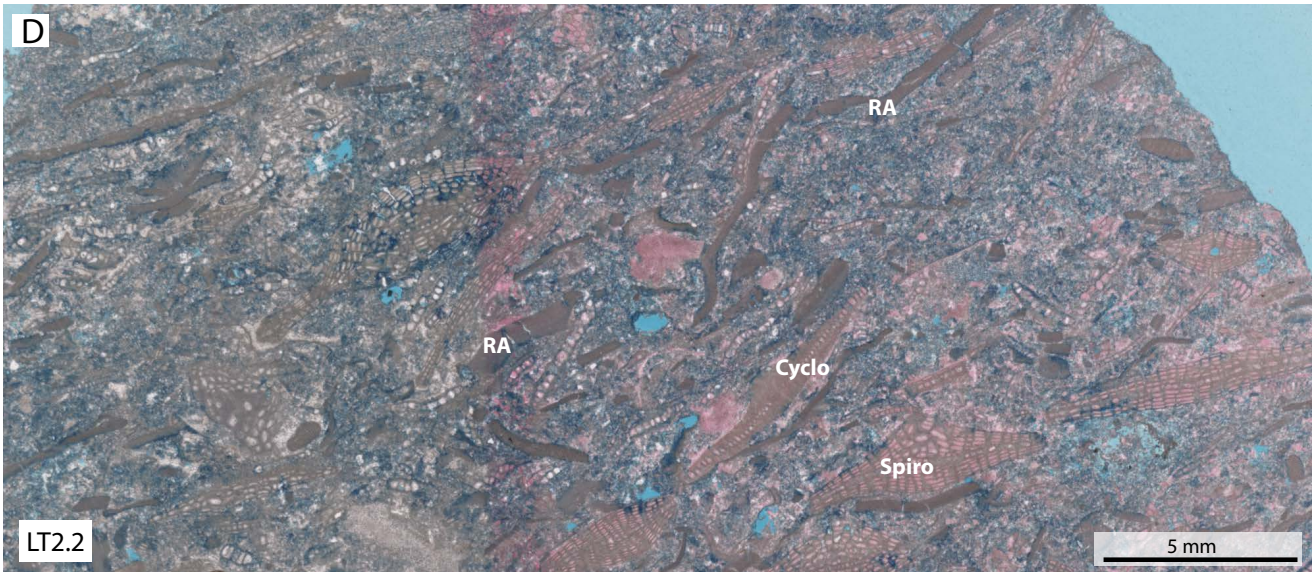
D
RA
RA
Cyclo
Spiro
LT2.2
5 mm

Figure 8

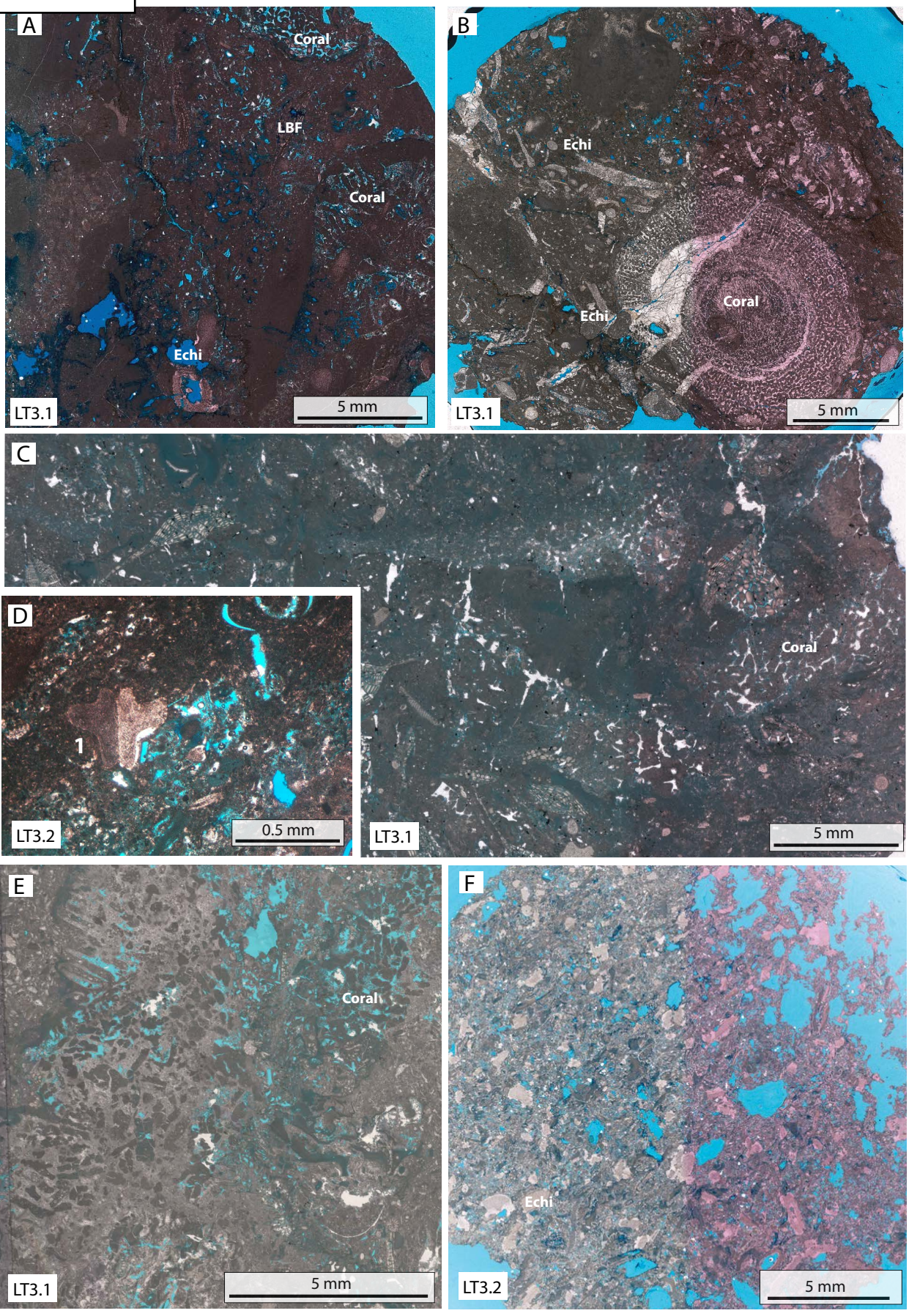
A
Coral
LBF
Coral
Echi
LT3.1
5 mm
B
Echi
Echi
Coral
LT3.1
5 mm
C
Coral
LT3.1
5 mm
D
1
LT3.2
0.5 mm
E
Coral
LT3.1
5 mm
F
Echi
LT3.2
5 mm

Figure 9

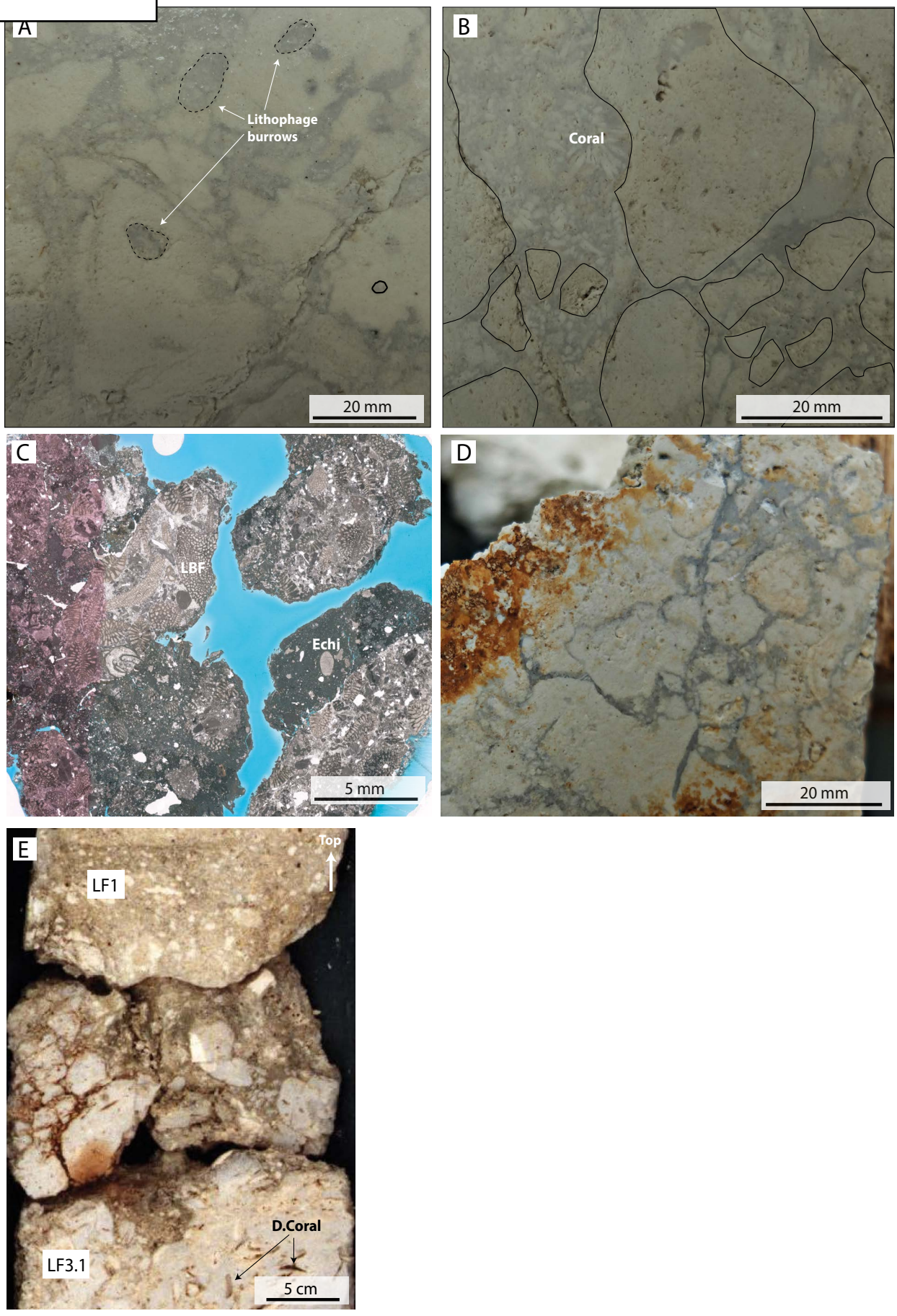
A
Lithophage burrows
20 mm
B
Coral
20 mm
C
LBF
Echi
5 mm
D
20 mm
E
Top
LF1
D.Coral
LF3.1
5 cm

Figure 10

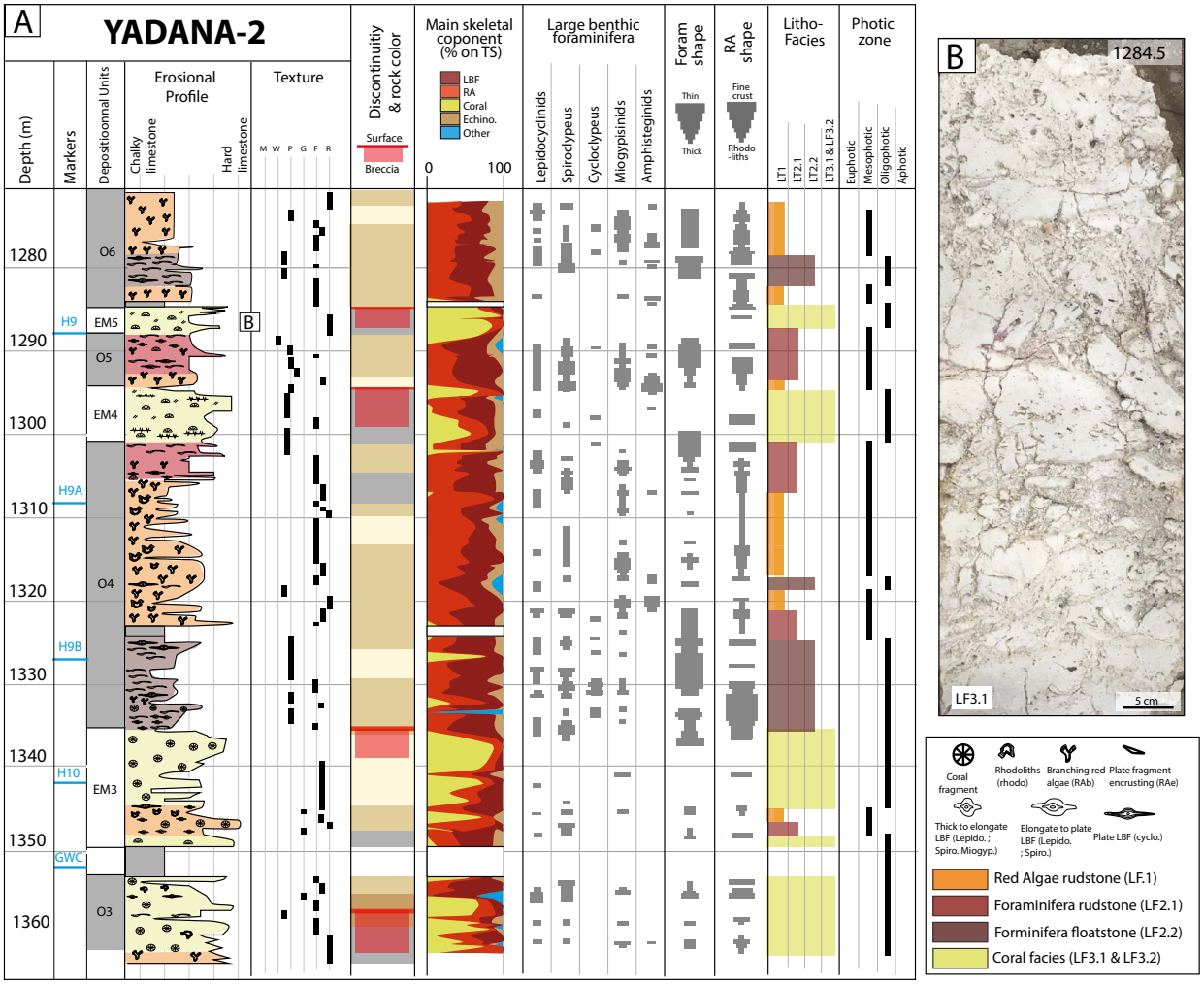
A
YADANA-2
Depth (m)
Markers
Depositioonnal Units
Erosional Profile
Chalky limestone
Hard limestone
Texture
M W P G F R
Discontinuity & rock color
Surface
Breccia
Main skeletal coponent (% on TS)
LBF
RA
Coral
Echino.
Other
0
100
Large benthic foraminifera
Lepidocyclinids
Spiroclypeus
Cyclociypeus
Miogypisinids
Amphisteginids
Foram shape
Thin
Thick
RA shape
Fine crust
Rhodo -liths
Litho-Facies
LT1
LT2.1
LT2.2
LT3.1 & LF3.2
Photic zone
Euphotic
Mesophotic
Oligophotic
Aphotic
1280
1290
1300
1310
1320
1330
1340
1350
1360
O6
EM5
O5
EM4
O4
EM3
O3
H9
H9A
H9B
H10
GWC
B
B
1284.5
LF3.1
5 cm
Coral fragment
Rhodoliths (rhodo)
Branching red algae (RAb)
Plate fragment encrusting (RAe)
Thick to elongate LBF (Lepido. ; Spiro. Miogyp.)
Elongate to plate LBF (Lepido. ; Spiro.)
Plate LBF (cyclo.)
Red Algae rudstone (LF.1)
Foraminifera rudstone (LF2.1)
Forminifera floatstone (LF2.2)
Coral facies (LF3.1 & LF3.2)
C
YADANA-3
Depth (m)
Markers
Erosional Profile
Chalky limestone
Hard limestone
Texture
M W P G F R B Brec
Discontinuity & rock color
Surface
Breccia
Main skeletal coponent (% on TS)
LBF
RA
Coral
Echino.
Other
0
100
Large benthic foraminifera
Lepidocyclinids
Spiroclypeus
Cyclociypeus
Miogypisinids
Amphisteginids
Foram shape
Thin
Thick
RA shape
Fine crust
Rhodo -liths
Litho-Facies
LT1
LT2.1
LT2.2
LT3.1 & LF3.2
Photic zone
Euphotic
Mesophotic
Oligophotic
Aphotic
1300
1310
1320
1330
1340
1350
O6
EM5
O5
EM4
O4
EM3
H9
H9A
H9B
GWC
H10
D
D
LF2.1
LF3.1
5 cm

Figure 11

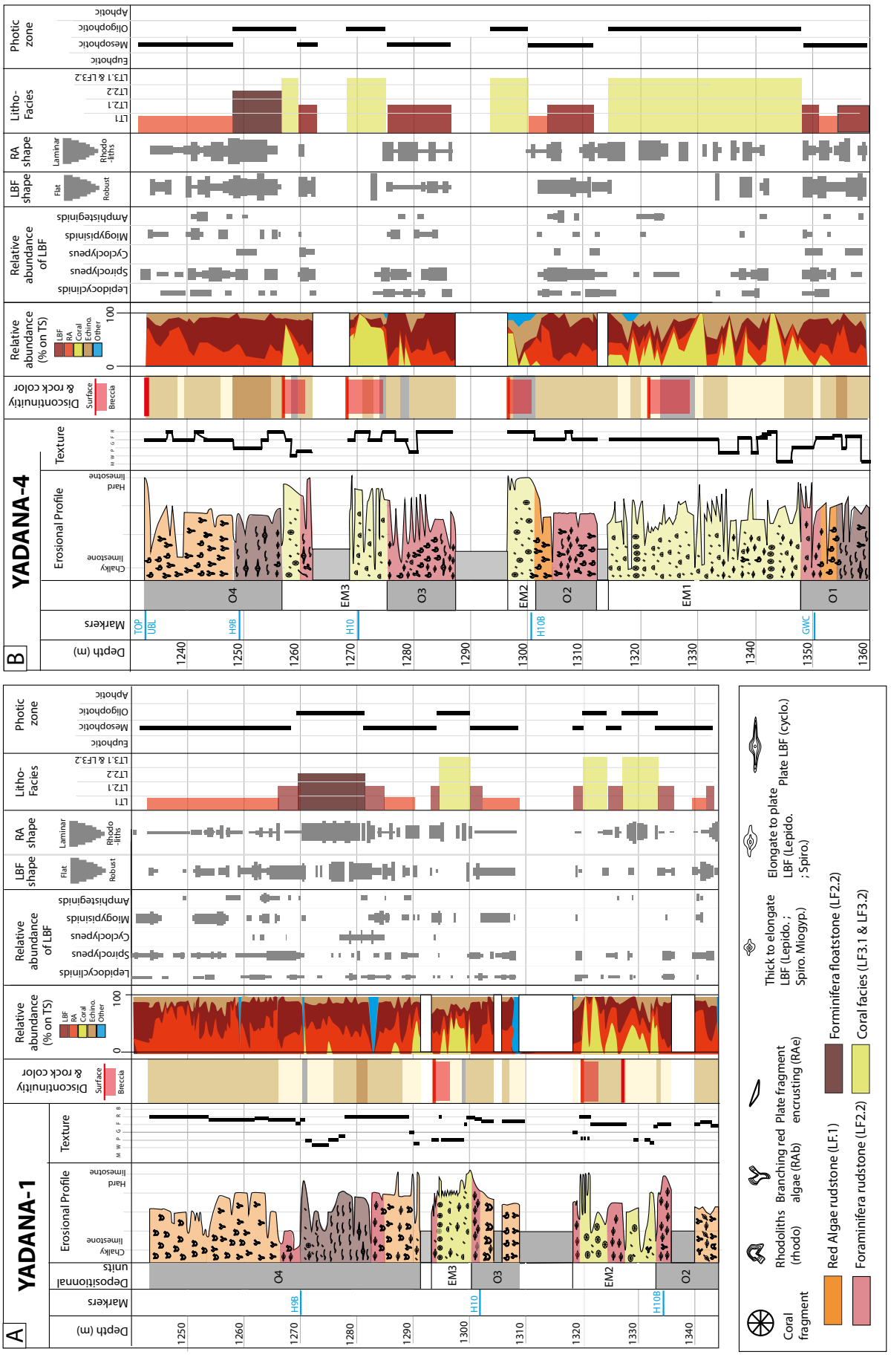
A
YADANA-1
B
YADANA-4
Depth (m)
Markers
Depositional units
Erosional Profile
Chalky limestone
Hard limestone
Texture
Discontinuity & rock color
Surface
Breccia
Relative abundance (% on TS)
LBF
RA
Coral
Echino.
Other
Relative abundance of LBF
Lepidocyclinids
Spirocyclypeus
Cyclocyclypeus
Miogypsinids
Amphisteginids
LBF shape
Flat
Robust
RA shape
Laminar
Rhodo-liths
Litho-Facies
LT1
LT2.1
LT2.2
LT3.1 & LF3.2
Photic zone
Euphotic
Mesophotic
Oligophotic
Aphotic
TOP
UBL
H98
H10
H10B
GWC
O4
EM3
O3
EM2
O2
EM1
O1
Coral fragment
Rhodoliths (rhodo)
Branching red algae (RAb)
Plate fragment encrusting (RAe)
Thick to elongate LBF (Lepido. ; Spiro. Miogyp.)
Elongate to plate LBF (Lepido. ; Spiro.)
Plate LBF (cyclo.)
Red Algae rudstone (LF.1)
Foraminifera floatstone (LF2.2)
Foraminifera rudstone (LF2.2)
Coral facies (LF3.1 & LF3.2)

Figure 12

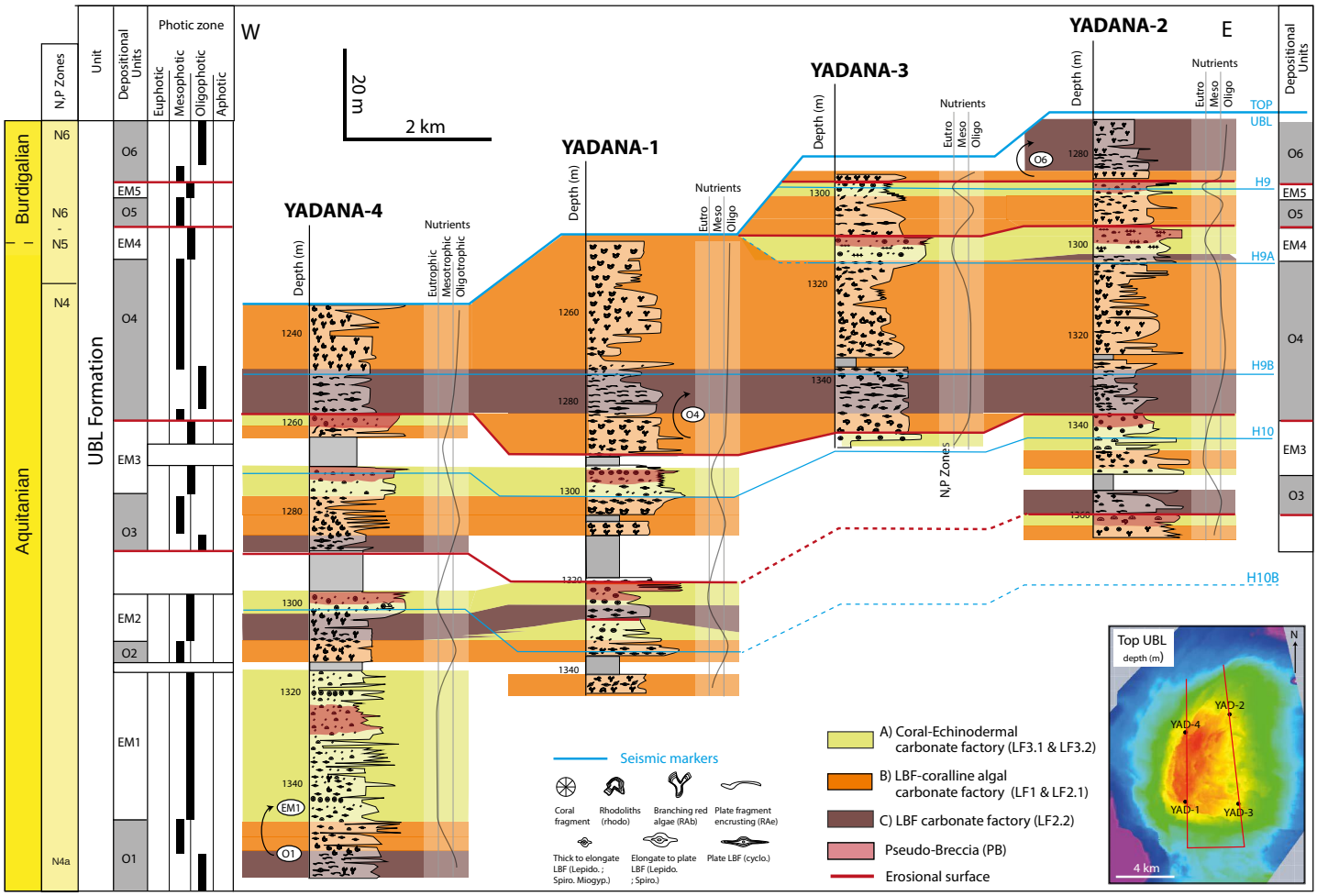
W
E
20 m
2 km
YADANA-4
YADANA-1
YADANA-3
YADANA-2
Depth (m)
Nutrients
Eutrophic
Mesotrophic
Oligotrophic
Eutro
Meso
Oligo
N,P Zones
Photic zone
Euphotic
Mesophotic
Oligophotic
Aphotic
Unit
Depositional Units
UBL Formation
Burdigalian
Aquitanian
N6
N6 - N5
N4
N4a
O6
EM5
O5
EM4
O4
EM3
O3
EM2
O2
EM1
O1
TOP UBL
H9
H9A
H9B
H10
H10B
Seismic markers
Coral fragment
Rhodoliths (rhodo)
Branching red algae (RAb)
Plate fragment encrusting (RAe)
Thick to elongate LBF (Lepido. ; Spiro. Miogyp.)
Elongate to plate LBF (Lepido. ; Spiro.)
Plate LBF (cyclo.)
A) Coral-Echinodermal carbonate factory (LF3.1 & LF3.2)
B) LBF-coralline algal carbonate factory (LF1 & LF2.1)
C) LBF carbonate factory (LF2.2)
Pseudo-Breccia (PB)
Erosional surface
Top UBL
depth (m)
YAD-2
YAD-4
YAD-1
YAD-3
4 km

Figure 13

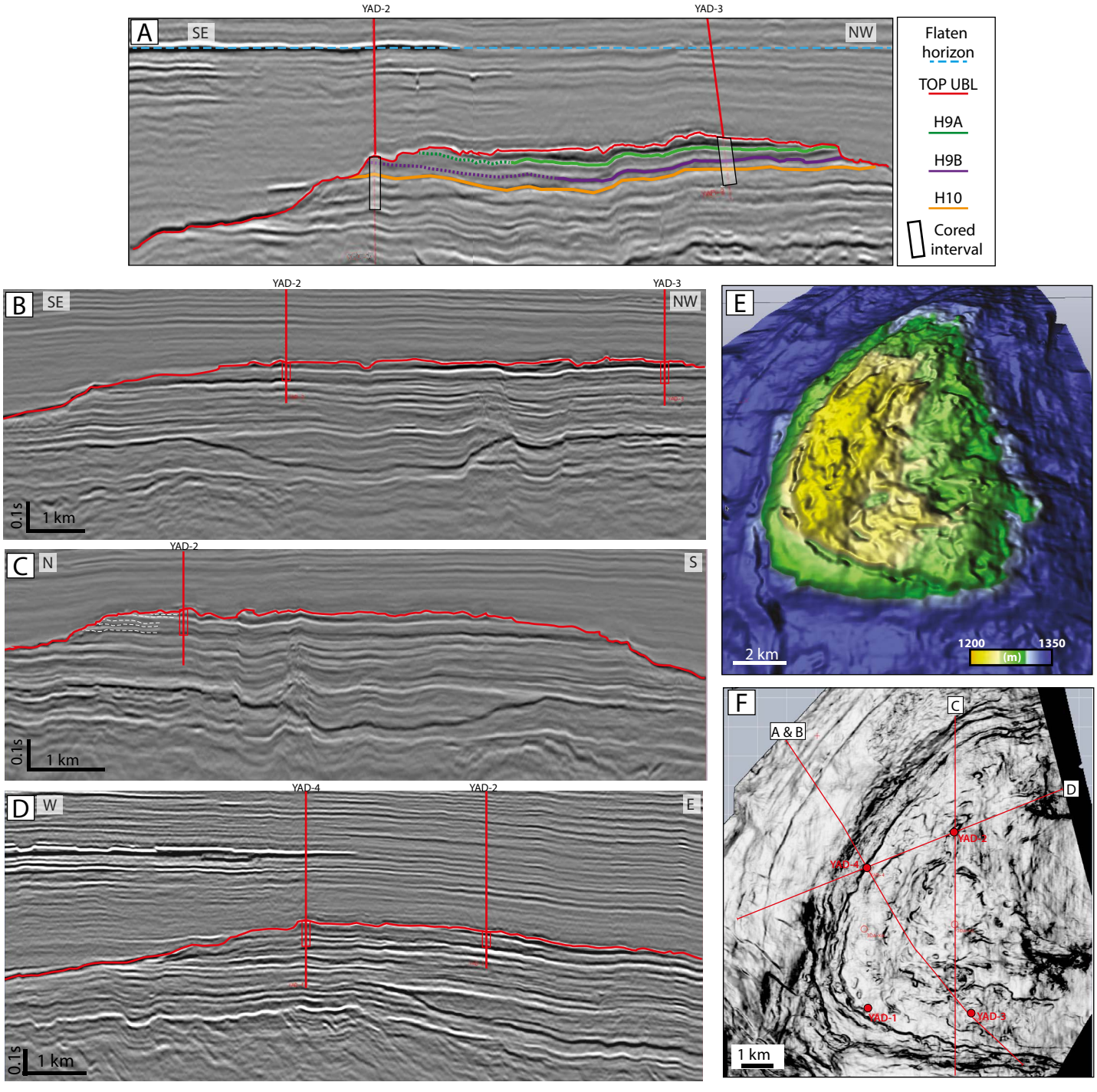
A
SE
NW
YAD-2
YAD-3
Flaten horizon
TOP UBL
H9A
H9B
H10
Cored interval
B
SE
NW
YAD-2
YAD-3
0.1s
1 km
C
N
S
YAD-2
0.1s
1 km
D
W
E
YAD-4
YAD-2
0.1s
1 km
E
2 km
1200
1350
(m)
F
A & B
C
D
YAD-2
YAD-4
YAD-1
YAD-3
1 km

Figure 14

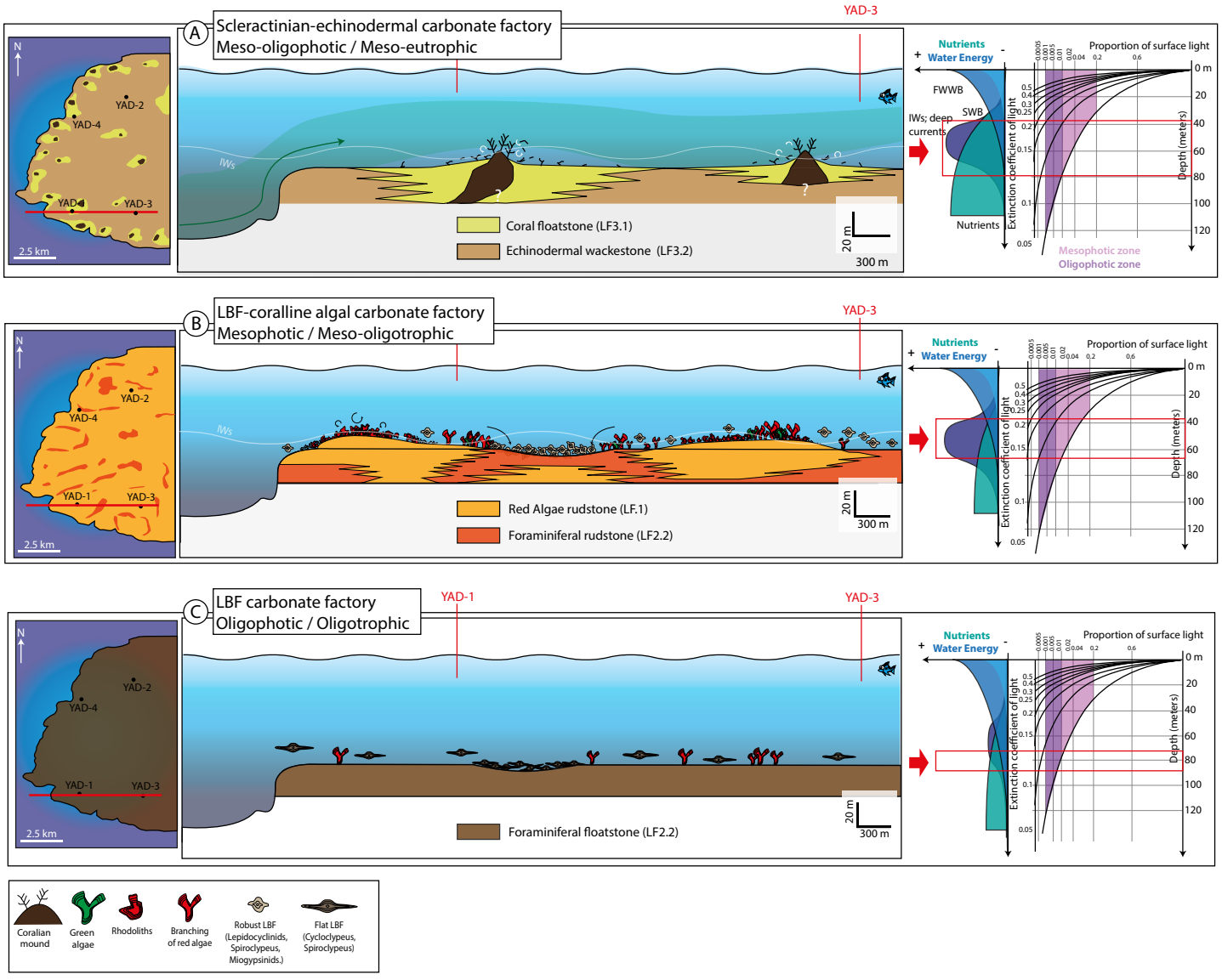
A
Scleractinian-echinodermal carbonate factory
Meso-oligophotic / Meso-eutrophic
YAD-3
N
YAD-2
YAD-4
YAD-1
YAD-3
2.5 km
IWs
Coral floatstone (LF3.1)
Echinodermal wackestone (LF3.2)
20 m
300 m
Nutrients
Water Energy
Proportion of surface light
FWWB
SWB
IWs; deep currents
Nutrients
Extinction coefficient of light
Depth (meters)
Mesophotic zone
Oligophotic zone
B
LBF-coralline algal carbonate factory
Mesophotic / Meso-oligotrophic
Red Algae rudstone (LF.1)
Foraminiferal rudstone (LF2.2)
C
LBF carbonate factory
Oligophotic / Oligotrophic
Foraminiferal floatstone (LF2.2)
Coralian mound
Green algae
Rhodoliths
Branching of red algae
Robust LBF (Lepidocyclinids, Spiroclypeus, Miogypsinids.)
Flat LBF (Cycloclypeus, Spiroclypeus)